ΔNp63 controls stemness and inflammation in the adult epidermis

Christopher E. Eyermann[1,2], Xi Chen[1,2], Ozge S. Somuncu[1,2], Jinyu Li[1,2], Alexander N. Joukov[3], Jiang Chen[1,2], Evguenia M. Alexandrova[1,2]*

[1]Department of Pathology, Stony Brook University, Stony Brook, NY, USA, [2]Stony Brook Cancer Center, Stony Brook, NY, USA, [3]Ward Melville High School, East Setauket, NY, USA

*Author for correspondence, email: evguenia.alexandrova@stonybrook.edu

ABSTRACT

The p63 transcription factor is critical for epidermis formation in embryonic development, but its role in the adult epidermis is barely investigated. Here we show that acute genetic ablation of ΔNp63, the main p63 isoform, in the adult epidermis disrupts keratinocyte proliferation and self-maintenance and, unexpectedly, triggers an inflammatory psoriasis-like condition. Mechanistically, single-cell RNA sequencing revealed down-regulation of the cell cycle genes, up-regulation of differentiation markers, and induction of several pro-inflammatory pathways in ΔNp63-ablated keratinocytes. Intriguingly, ΔNp63-ablated cells disappear three weeks post-ablation, at the expense of the remaining non-ablated cells. This was not associated with active cell death mechanisms, but rather with reduced stemness and self-maintenance capacity. Indeed, *in vivo* wound healing assay, a physiological readout of the epidermal stem cell function, was largely impaired in the ablated skin. We found that the Wnt signaling pathway (Wnt5a, Wnt10a, Fzd6, Fzd10) and Col17a1 are the likely ΔNp63 effectors responsible for keratinocyte proliferation and stemness, while AP1 factors are responsible for excessive differentiation, and Il-1a, Il-18, Il-24 and Il-36γ for the suppression of inflammation. These data implicate ΔNp63 as a critical node that coordinates balanced epidermal homeostasis and suppression of inflammation in the adult epidermis, upstream of known regulatory pathways.

INTRODUCTION

Skin, the largest organ of the body, serves as an essential protective barrier against the hostile environment, prevents moisture escape, and ensures body integrity. Its outermost layer, the epidermis, is responsible for the skin barrier function and is composed of the main cell type, keratinocytes (KCs). One of the major regulators of the epidermis in embryonic development (morphogenesis) is the *p63* gene (1), whose knockout (KO) results in severe defects of the epidermis and its appendages, resulting in perinatal lethality (2, 3). The *p63* gene produces multiple N- and C-terminal isoforms, the main class being the full-length TAp63 and the N-terminally truncated ΔNp63 isoforms transcribed from an alternative internal promoter (4). ΔNp63 is the principal p63 isoform, evident by its significantly higher expression in the epidermis than TAp63 (2, 4-6) and by the phenotypes of ΔNp63-KO embryos that greatly mimic global p63 KOs, i.e., lacking all isoforms (2, 3, 7, 8). The severe epidermal defects in p63 and ΔNp63-KO embryos have been attributed to either impaired epidermal stem cell (SC) maintenance (2, 7, 9, 10) or defective KC commitment and differentiation (3, 11-14). Notably, p63 and ΔNp63 continue to be strongly expressed in the adult epidermis and there, in the basal/supra-basal gradient consistently with the epidermal SC niche (4, 15, 16). However, their role in the mature epidermis remains obscure, primarily due to the perinatal lethality of KOs (2, 3, 7, 8). Thus, conditional knockout of p63 (all isoforms) in adult mice promotes aging and induces senescence markers in the skin (17). However, it is unclear how the aging phenotype relates to the skin defects and which p63 isoforms are involved, especially given concerns about this model's reliability (18). Furthermore, previous studies of ΔNp63-specific knockdown (KD) in the adult skin revealed conflicting data, e.g., epidermal hypo-proliferation in a regenerating human epidermis model (12), but hyper-proliferation in siRNA-mediated *in vivo* KD mice (14). In humans, mutations in the *p63* gene are associated with rare familial EEC (ectrodactyly, ectodermal dysplasia, cleft lip/palate) and other skin fragility syndromes, highlighting a critical role of p63/ΔNp63 in the adult skin (19). In addition, p63/ΔNp63 is overexpressed in squamous cell carcinomas where it acts as an oncogenic driver (15, 16, 20, 21). In contrast, TAp63 plays a milder role in skin aging, non-epithelial tissues, and as a tumor suppressor (22-26). Genomic and epigenetic analyses indicate a broad role of p63/ΔNp63 as a chromatin modifier and a transcription factor that can both, activate and a repress its targets, despite lacking the classical transactivation (TA) domain in ΔNp63 (27-31). Here, we addressed the role of ΔNp63 in the adult epidermis

using a conditional KO mouse model, ΔNp63$^{fl/fl}$;K14-CreT2 mice. We found that ΔNp63 plays at least two critical roles in the adult epidermis. First, it regulates epidermal homeostasis (the balance of KC proliferation and differentiation) and SC maintenance. Second, quite unexpectedly, it keeps in check the KC-specific pro-inflammatory program. This establishes ΔNp63 as the master regulator of the adult epidermis, similar to (and beyond) its previously demonstrated embryonic roles.

RESULTS

The phenotype of ΔNp63-ablated mice

To investigate the role of ΔNp63 in the adult epidermis *in vivo*, we combined previously described ΔNp63^{fl} (8, 28, 32) and Krt14-CreERT2 (hereafter, K14-CreT2) alleles (33) to generate conditionally inducible ΔNp63$^{fl/fl}$;K14-CreT2 mice, as well as two control cohorts: ΔNp63$^{fl/fl}$ (no Cre recombinase) and ΔNp63$^{fl/+}$;K14-Cre (for heterozygous ablation) (Figure 1a). This allows for Tamoxifen induced ΔNp63 ablation in the basal epidermal layer, its predominant expression site. Upon Tamoxifen exposure, *ΔNp63* and *total p63* mRNA levels were significantly reduced in the skin of ΔNp63$^{fl/fl}$;K14-CreT2, but not control mice, while *TAp63* was slightly upregulated (Figure 1b). Compensatory *TAp63* upregulation was previously noted in ΔNp63-depleted cells (12, 17, 32), but due to its very low expression compared to *ΔNp63* (2, 4-6), its impact is probably minor. Furthermore, p63 protein expression (in lieu of ΔNp63) was greatly reduced the interfollicular epidermis (Figure 1c), but not so much in the hair follicles, likely due to their weaker Krt14 expression (34). Phenotypically, ΔNp63-ablated mice frequently developed patchy - and temporary - alopecia (hair loss, 77%) (Figure 1d, e; Supplementary Table 1), as well as temporarily loss of body weight (up to 20-25%, Figure 1f; Supplementary Figure 1a, b).

Histopathology was essentially normal at 1 day, but revealed numerous defects at 1 wk post-ablation: acanthosis (epidermal thickening), hyperkeratosis (thickened cornified layer indicative of excessive keratin production and shedding), enlarged keratohyalin granules, parakeratosis (aberrant shedding of nucleated cells), and changes in the dermis: fibrosis, immune cell infiltration, hyperplasia of the sebaceous glands (Figure 2a-e; Supplementary Figure 1c, d). This phenotype is consistent with skin inflammation and resembles psoriasis vulgaris in humans, except for hyperplastic sebaceous glands (hypoplastic in psoriasis) (35). While alopecia may or may not accompany psoriasis in humans (35, 36), since alopecic ("bald") areas strongly

correlate with the most aberrant histopathology in our mice (Figure 2c; Supplementary Figure 1c), this is likely not a separate phenotype.

Notably, ΔNp63 mRNA and protein expression and skin histopathology were largely restored by 3 wks post-ablation, followed by reversal of alopecia at 4 wks (Figure 1b, c, e; Figure 2e). This points to a rapid loss of ΔNp63-ablated basal KCs, likely due to expansion of the remaining non-ablated KCs, and suggests their reduced self-maintenance. We speculate that if the ablation efficiency was close to 100%, this would be incompatible with the existence of the epidermal layer, similarly to p63/ΔNp63-KO embryos (2, 3, 7, 8).

Proliferation and self-maintenance defects in ΔNp63-ablated epidermis

Epidermal thickening (acanthosis) in ΔNp63-ablated mice suggests increased KC proliferation. Indeed, Ki67 staining revealed overall hyper-proliferation at 1 wk post-ablation, but not at 1 day or 3 wks (Figure 2f, g; Supplementary Figure 1e, f), which contradicts many reports of that p63/ΔNp63 is required for KCs proliferation or proliferative potential (7, 9, 10, 12, 15). However, serial sections revealed that hyper-proliferation is mostly confined to the remaining non-ablated (ΔNp63^{pos}) KCs, while ΔNp63^{neg} KCs remain hypo-proliferative (Figure 2h, i). In agreement, the dissected alopecic ("bald") skin patches were always both, Ki67^{pos} and p63^{pos} (Figure 2j). This suggests that ΔNp63 ablation non-cell-autonomously induces proliferation in the remaining ΔNp63^{pos} KCs, e.g., via secreted pro-inflammatory cytokines (see below).

Rapid loss of ΔNp63^{neg} KCs suggests two possibilities: (1) the ablated KCs die, indicating that ΔNp63 is required for their survival or (2) the ablated KCs have impaired self-maintenance and become extinct via losing competition to the remaining - better fit - ΔNp63^{pos} KCs. We found no evidence of the former. Thus, necrosis (RIP3) and apoptosis (TUNEL, Cleaved Caspase-3) markers were only slightly increased, which was not statistically significant and, importantly, they localized to the outermost, not the basal ΔNp63-ablated KCs (Supplementary Figure 2 and *not shown*), the cell death pattern characteristic for psoriatic KCs (37). Likewise, the markers of cellular senescence (SA-X-gal, p16) were not induced (*not shown*). Altogether, these data indicate that ΔNp63 is required for KC self-maintenance and optimal fitness rather than survival.

Molecular pathways altered in ΔNp63-ablated epidermis

To gain insight into the molecular mechanisms of the observed defects, we performed single-cell RNA sequencing (scRNA-seq) analysis of ΔNp63-ablated vs. control KCs at 1 day and 1 wk post ablation (from n=3 pooled mice each). At 1 day post-ablation, two distinct KC populations were found in ΔNp63-ablated epidermis: (1) with a gene expression signature similar to control KCs (average *p63* mRNA expression=0.36 of control) and (2) with a completely new gene expression signature (*p63* mRNA=0.18 of control), which we termed $p63^{med}$ and $p63^{low}$ clusters, respectively (Figure 3a; Supplementary Figure 3a, b). Similarly, at 1 wk post-ablation, only some KCs had a gene expression signature similar to control KCs, while the majority had a distinct gene expression signature, therefore, we termed them "Normal-like" and "Hyper-proliferative" clusters, respectively (Figure 3b; Supplementary Figure 3a, b, see Ki67). Notably, *p63* expression likely reflects the *ΔNp63* isoform (not directly detectible by scRNA-seq), since known ΔNp63 target genes were down-regulated, while TAp63 target genes were upregulated in ΔNp63-depleted cells (Figure 3c; Supplementary Figure 3c).

Analysis of differentially expressed genes and the Reactome pathways at the earliest time-point, 1 day post-ablation, revealed that the most significantly upregulated pathways in ΔNp63-ablated KCs are: (1) "Keratinization" (including KC differentiation genes), (2) interleukin signaling (the Il-1, Il-4/13, Il-10, Il-36 pathways) and (3) the Nerve Growth Factor (NGF) pathway (Figure 3d). The latter two are linked to inflammatory skin conditions, e.g., psoriasis and atopic dermatitis (AD) (38-41). The most down-regulated pathways shared by $ΔNp63^{low}$ and $ΔNp63^{med}$ clusters were the cell-cell and cell-ECM (extracellular matrix) interaction pathways (Figure 3e), consistently with previous reports of p63/ΔNp63 regulation of cell-cell and cell-ECM adhesion (1, 14, 21, 42, 43). Strikingly, $ΔNp63^{low}$ and $ΔNp63^{med}$ clusters showed an opposite regulation of the cell cycle genes and previously identified "core" stemness genes (44): down-regulation in $ΔNp63^{low}$ and upregulation in $ΔNp63^{med}$ (Figure 3d, e, *red boxes,* Supplementary Figure 4a). This independently confirms that ΔNp63-ablated KCs are hypo-proliferative with reduced stemness/self-maintenance capacity, while the remaining $ΔNp63^{pos}$ KCs (likely in the $p63^{med}$ cluster) are hyper-proliferative with increased stemness, in agreement with our Ki67 analysis (Figure 2h-j). ScRNA-seq analysis of a later time-point, 1 wk post-ablation, revealed similar pathway changes, except for a widespread upregulation of the cell cycle pathways exclusively in the "Hyper-proliferative" cluster (hence its name; Supplementary Figure 4b, c), suggesting that this cluster represents the expanded "psoriatic" KCs. Overall, scRNA-seq has revealed in

an un-biased way four major molecular defects in ΔNp63-ablated adult epidermis: impaired proliferation of the most depleted KCs, enhanced terminal differentiation (together, imbalanced homeostasis), broad upregulation of the inflammatory program, and reduced cell-cell and cell-ECM interactions.

Differentiation and stratification defects in ΔNp63-ablated epidermis

ScRNA-seq revealed expansion of the granular/differentiated cluster in ΔNp63-ablated epidermis at both, 1 day and 1 wk post-ablation (Figure 3a, b, *purple*), and upregulation of the "Keratinization" pathways (Figure 3d; Supplementary Figure 4b), consistently with the observed hyperkeratosis and increased keratohyalin production (Figure 2a-c). Indeed, analysis of individual stratification markers showed upregulation of many differentiation genes: *Flg*, *Tgm1/3/5*, *Klk5-12*, while the basal marker *Krt5*, a ΔNp63 target gene (5), was reduced (Figure 4a, b). This was confirmed by qRT-PCR and immunofluorescent staining (Figure 4c, d; Supplementary Figure 5a-c, h). Surprisingly, basal *Krt14* (also reportedly a ΔNp63 target gene (5, 45) was not significantly reduced at 1 day and even up-regulated at 1 wk post-ablation (Figure 4a, b), and its protein expression showed expansion into supra-basal layers and an overlap with the spinous and granular layer markers Krt10 and Lor, respectively (Figure 4e, f), indicating aberrant epidermal stratification. Furthermore, ΔNp63-depleted KCs were previously shown to spontaneously reprogram into induced pluripotent stem cells (iPSC) via a micro-RNA processing factor DGCR8 (8). Therefore, we assessed expression of *DGCR8*, as well as iPSC and embryonic markers. We found a marked aberrant upregulation of embryonic *Krt8/18,* similarly to previous reports in late p63/ΔNp63-depleted embryos (7, 8, 12, 13, 27), but no induction of iPSC genes, and only minor down-regulation of *DGCR8* at the late 1 wk time-point (Figure 4a, b, g; Supplementary Figure 5d-g). This indicates that DGCR8 is not a major ΔNp63 effector in the adult epidermis. Altogether, these data indicate a critical role of ΔNp63 in restraining excessive terminal differentiation and suppressing immature keratin genes in the adult epidermis.

ΔNp63 effectors responsible for epidermal homeostasis

Many genes and pathways are known to regulate epidermal homeostasis, e.g., the Wnt/β-catenin and Shh pathways - KC proliferation, stemness, maintenance (46, 47); AP1 (aka Jun/Fos) and the Notch pathway -

KC differentiation (48, 49). Analysis of these and other signaling pathways, including those proposed to be regulated by p63/ΔNp63 (21, 27, 30), revealed significant down-regulation of the Wnt pathway (Figure 5a, d), as well as Shh and Edaradd pathway components in the most ablated ΔNp63^{low} cluster (Supplementary Figure 6a). In addition, *Collagen 17a1* (*Col17a1*) from the cell-ECM interaction pathways, a gene known to regulate KC proliferation and stemness and previously implicated as a ΔNp63 target in squamous cell carcinoma (21, 50-52), was strongly down-regulated (>4 folds, Figure 5b, f). On the contrary, several AP1 transcription factors were strongly upregulated (Figure 5c, e). All other signaling pathways, e.g., Notch, FGF, TGFβ previously proposed to mediate ΔNp63 functions, were either not affected or showed concomitant up- and down-regulation (Supplementary Figure 6a). Furthermore, comparison of the genomic sequences/epigenetic regulatory tracks in the UCSC Genome Browser with a published p63 ChIP-seq database (31) revealed potential p63 binding sites in several Wnt pathway components (*Fzd6, Fzd10, Wnt5a, Wnt10a*), *Col17a1*, and several AP1 genes (*Fos, Fosb, Fosl2/Fra1, JunB*, Figure 5g, h; Supplementary Figure 6b, c). Since ΔNp63 can both, activate and repress its target genes (27, 28), these data strongly suggest that ΔNp63 coordinates epidermal homeostasis by activating the pro-proliferative/pro-stemness Wnt pathway and *Col17a1*, while repressing the differentiation driving AP1 factors.

Impaired wound healing in ΔNp63-ablated skin

One physiologically important role of epidermal SCs is to facilitate wound repair (53). Therefore, we tested whether reduced stemness of ΔNp63-ablated KCs would affect their wound healing capacity. To this end, we introduced two bilateral full-skin excision wounds via a 6 mm biopsy punch at 1 day post-ablation. We found that, indeed, wound healing was severely impaired in ΔNp63-ablated mice (Figure 6a, b). This was accompanied by failure to form the hyper-thickened epidermal ridge, despite the aforementioned acanthosis away from the wound (Figure 6c, d), and failure to induce Col17a1 (Figure 6e), consistently with reduction of its mRNA expression (Figure 5b). Notably, proliferation near the wound was not affected (Figure 6f, g) and was increased away from the wound as noted before (acanthosis, Figure 2a). Strikingly, the non-ablated p63^{pos} cells failed to migrate towards the wound (Figure 6h) as one might expect from other incomplete KOs (54). This reveals a dominant-negative effect of ΔNp63^{neg} KCs towards ΔNp63^{pos} KCs, which we speculate is due to

defective cell-ECM interaction pathways (Figure 3e; Supplementary Figure 4c, *yellow*). Overall, the wound healing assay has revealed a critical, physiologically relevant role of ΔNp63 as a SC regulator in the adult epidermis.

Regulation of inflammation by ΔNp63

Consistently with the inflammatory phenotype (Figure 2a, c), scRNA-seq revealed upregulation of several interleukin pathways: Il-1, Il-4/13, Il-10, Il-36, and the NGF pathway, all associated with inflammatory diseases, e.g., psoriasis and AD (38-41) (Figure 7a, b; Supplementary Figure 7a). In addition, many epidermis-specific "alarmin" genes were upregulated: *Krt6a/b, Krt16/17*, *Lce3c-f*, *s100a8/9*, *Slurp1/2*, *Sprr1/2*, also associated with psoriasis and occasionally with AD (55-60) (Figure 7c). Notably, several lines of evidence point to a psoriasis-like rather than AD-like condition in ΔNp63-ablated mice: upregulation of *Il-1*, *Il-36* and *s100a8/9* (higher in psoriasis than AD (60, 61)), "hallmark of psoriasis" *Krt6/16/17* genes (55), increased differentiation/cornification (reduced in AD), characteristic parakeratosis, and upregulation of *Tnf* and *Ifngr1/2* genes (Supplementary Figure 7a) (40, 41, 58, 59, 62). Moreover, our analysis of the biopsies of human plaque psoriasis revealed protein expression patterns similar to those in ΔNp63-ablated mouse skin: Il-36α upregulation and localization in the outermost layer (Figure 7d, e), Krt14 expansion into supra-basal layers and overlap with spinous and granular markers Krt10 and Lor, respectively, and reduced Flg expression (37) (Figure 7f-h, compare to Figure 4d-f). This suggests that ΔNp63 is an epidermis-specific negative regulator of psoriatic inflammation. Indeed, analysis a p63 CHIP-seq database (31) revealed potential p63 binding sites in several cytokines and cytokine receptors from the upregulated inflammatory pathways: *Il-1a* (a previously established ΔNp63 target (63)), *Il-18*, *Il-24, Il-36γ,* and *Ifng1/2* (Figure 7i, j; Supplementary Figure 7b, c and *not shown*) - all implicated in skin psoriasis in humans (38, 62-67). Furthermore, we found a significantly decreased number of p63^{pos} KCs in human psoriatic biopsies compared to normal and non-lesional skin (Figure 7k, l), as previously reported (68-70). In sum, one of novel unexpected functions of ΔNp63 in the adult skin - not inferred from previous embryonic and *in vitro* studies - is repression of a KC-specific pro-inflammatory program, likely via direct suppression of a number of cytokine and/or cytokine receptor genes.

DISCUSSION

Here we for the first time unequivocally established a critical role of ΔNp63 in the adult epidermis in an *in vivo* genetic model (Figure 8). Specifically, we found that ΔNp63 (1) promotes proliferation, maintenance and stemness of basal KCs, via the Wnt pathway and *Col17a1*, physiologically revealed by the wound healing assay; (2) suppresses terminal differentiation, via repression of the AP1 factors; and (3) suppresses KC-specific inflammatory program, via repression of pro-inflammatory cytokines (Figure 8a). In ΔNp63-ablated epidermis, all these functions are curtailed, resulting in multiple concomitant defects (Figure 8b). Notably, it is still debatable whether the epidermal defects of p63 and ΔNp63-KO embryos are due to defective KC maintenance (2, 7, 9, 10) or differentiation/stratification (3, 11-14). Our data strongly support the former, at least in the adult skin. Similarly, there is an ongoing debate whether p63/ΔNp63 depletion reduces (7, 9, 12) or increases KC proliferation (8, 14), including in the adult models. Our analyses indicate that ΔNp63-depleted KCs are hypo-proliferative, while the remaining non-ablated KCs are hyper-proliferative, likely in response to the paracrine inflammatory signals from the depleted KCs. This suggests that the previous reports of KC hyper-proliferation also deal with an incomplete KD. Regarding another intriguing phenotype of ΔNp63-ablated mice, loss of body weight, we have excluded defects in the esophagus and tongue that might cause malnutrition (in fact, p63 was not downregulated there; *data not shown*) and speculate the weight loss may be caused by dehydration due to impaired skin barrier function, which we are currently investigating.

Several signaling pathways downstream of ΔNp63 were proposed in embryonic epidermis and adult KCs: Wnt, Notch, FGF and Eda, while the AP2-AP1 axis was proposed to be ΔNp63-independent (27, 30). Indeed, our data in the adult epidermis strongly support the role of the Wnt (and possibly, Shh and Eda), but not other signaling pathways, as well as AP1 (Jun/Fos) downstream of ΔNp63. Interestingly, while the same Wnt receptors were implicated as ΔNp63 targets in embryonic KCs (*Fzd6, Fzd10*), we found distinct Wnt ligands involved: *Wnt5a* and *Wnt10a*, as opposed to *Wnt3a, Wnt4, Wnt7b* and *Wnt10b* in the embryos, as well as *Lef1* and *β-catenin* (27). In addition, we propose that Col17a1, a transmembrane protein localized to the dermal surface of the basal KCs, is a major ΔNp63 effector in the adult epidermis. Col17a1 is strongly down-regulated in ΔNp63-ablated epidermis at mRNA and protein levels, has p63 binding sites, and was previously shown to bind p63 in squamous cell carcinoma (21) and to potently regulate epidermal and hair follicle SCs,

while Col17a1-KO mice develop epidermal hyperplasia similar to our ΔNp63-ablated mice (50-52). As a hemidesmosomal component, Col17a1 may also mediate ΔNp63's role in the cell-ECM adhesion in the adult skin, one of our future research directions.

One novel unexpected function of ΔNp63 uncovered in this study is suppression of inflammation. Previously, ΔNp63 overexpression was shown to induce AD in mice (71-73) and to promote breast cancer via CXCL2 and CCL22 chemokines (74). In contrast, our data reveal that ΔNp63 suppresses - not promotes - a psoriasis-like epidermal inflammation. Psoriasis is a chronic autoimmune disease driven by an interplay between the immune system (Th1, Th17 cells and their effectors Il-17, Il-22, Il-23, TNF, IFN-γ) and epidermal KCs (62). However, this model postulating the primary role of the immune system has been challenged, e.g., by findings that psoriatic iPSC-derived KCs have inflammatory mRNA signatures in the absence of the immune cells (75). This indicates that epidermal mechanisms may be primary/epistatic to the immune system in driving psoriasis (62, 76). Our finding of a broadly upregulated inflammatory program in ΔNp63-ablated KCs immediately after ablation (likely prior to the immune cells involvement) supports this unconventional model. In agreement, we find reduced p63 expression in human psoriasis biopsies, consistently with previous reports of reduced expression of p63 protein, both *ΔNp63* and *TAp63* mRNAs, and ΔNp63 target genes in human psoriasis, and association of the *p63* genomic locus with psoriasis susceptibility (68-70).

In sum, we propose that ΔNp63 is the gatekeeper of adult epidermal homeostasis and regeneration and also, is critical to keep in check epidermal inflammation.

MATERIALS AND METHODS

Mouse strains, isolation of primary keratinocytes

ΔNp63$^{fl/fl}$ mice (8) and Krt14-CreT2 mice (Jackson Labs, Bar Harbor, ME, strain 005107) were previously described (33). They were inter-crossed to obtain the experimental and two control cohorts on a mixed 129SVJ/C57Bl6J/FVBN background. For ΔNp63 ablation, 2-17 m.o. animals received five doses of 200 mg/kg Tamoxifen (Sigma, Cat. # T5648-5G) in corn oil (Sigma, Cat. # C8267) via daily oral gavage. All animals were treated humanely and according to the guidelines by the Stony Brook University Institutional Animal Care and Use Committee. Males and females were used at 1:1 ratio, no differences were noted between the

genders or cohorts of different age. The sample size was not pre-determined. Animals were randomized into treatments. Primary mouse KCs were isolated as previously described (77) with slight modifications (see "Supplementary Material").

Wound healing assay

For *in vivo* wound healing assay, mice were anesthetized with Ketamine/Xylazine (60 mg/kg; 100 mg/kg, respectively, in 0.67% NaCl), their back skin was shaved and wiped with 70% ethanol, and two bilateral full-skin excision wounds were introduced with a sterile 6 mm biopsy punch, followed by mouse single housing on the MediGel-CPF diet/analgetic post-procedure. Two hrs prior to euthanasia, BrdU (Life Technologies, Carlsbad, CA, Cat. No. 000103) was i.p. injected according to the manufacturer's instructions. Epidermal thickness "Near wound" was the measured at the thickest site excluding hair follicles. $BrdU^{pos}$ and $Ki67^{pos}$ cells "Near wound" and "Away from wound" were counted in the first five interfollicular spaces next to the wound and in interfollicular spaces 7 to 12, respectively. Two spaced-out sections of each wound on both wound sides were analyzed (n=4 measurements per wound).

Quantitative RT-PCR, immunohistochemistry, immunofluorescent staining

Total RNA was extracted from whole back skin or from isolated KCs and qRT-PCR was performed as previously described (78). The PCR primers for total *p63*, Δ*Np63*, *TAp63* (18), *HPRT, Oct4*, *Sox2*, *Nanog* (79) were previously described. For additional primers, see "Supplementary Material". Immunohistochemistry (IHC) and immunofluorescent staining were done as previously described (78) with slight modifications, see "Supplementary Material" for details and the primary antibodies.

Single-cell RNA sequencing, genomics and pathway analyses

ScRNA-seq was performed at NYU Genome Technology Center as previously described (78), except that Chromium Next GEM Single Cell 5′ Library & Gel Bead Kit v1.1, PN-1000165 was used at 1 wk post-ablation, and K-mean clustering ($k = 10$) was used for dimensionality reduction at both timepoints. The pathway analysis was done using the Reactome tool (www.reactome.com) based on the differentially expressed genes

identified by scRNA-seq. For heatmaps, the genes with absolute expression levels <0.01 across the three assessed categories were excluded. Analysis of human genomic sequences and epigenetic regulatory tracks was done in UCSC Genome Browser, version GRCh37/hg19 (www.genome.ucsc.edu). The ENCODE function was used to detect H3K4Me3 (promoters), H3K4Me1 (inactive enhancers) and H3K27Ac (active enhancers) modifications in NHEK cells (normal human epidermal KCs). Genomic/epigenetic tracks were overlayed with a published CHIP-seq database of p63 binding sites in NHEK cells at Day 0 (proliferative condition) and Day 7 (differentiation condition) (31).

Statistical analysis

Unpaired two-tailed Student's *t*-test was used in all experiments, except scRNA-seq and Reactome analyses. Mean ± SD was plotted and $p<0.05$ was considered statistically significant. All experiments were performed in at least three biological replicas, unless indicated otherwise. No blinding was used. Normal distribution and variance between the groups was not tested for.

ACKNOWLEDGEMENTS

We wish to acknowledge the Stony Brook Cancer Center's shared resource facilities for tissue processing, sectioning and H&E staining (Histology Core Facility), providing biopsies of psoriasis and normal human skin (Biobank), and assistance with bioinformatics analysis (Biostatistics and Bioinformatics Core Facility). We are grateful to Dr. Elsa Flores for kindly providing $\Delta Np63^{fl/fl}$ mice, Dr. Ute Moll and Dr. Daniel Lozeau for assistance with skin histopathology, Hemma Kilawan for assistance with data analysis, NYU Genome Technology Center for performing scRNA-seq experiments, and Histowiz for assistance with IHC staining. EMA was supported by NIH grant K22CA190653 and by Stony Brook Cancer Center startup funds. JC was supported by NIH grant R01AR061485.

Conflict of Interest

Authors declare no conflict of interest.

REFERENCES

1. Guan Y, Yang YJ, Nagarajan P, Ge Y. Transcriptional and signalling regulation of skin epithelial stem cells in homeostasis, wounds and cancer. Exp Dermatol. 2021;30(4):529-45.
2. Yang A, Schweitzer R, Sun D, Kaghad M, Walker N, Bronson RT, et al. p63 is essential for regenerative proliferation in limb, craniofacial and epithelial development. Nature. 1999;398(6729):714-8.
3. Mills AA, Zheng B, Wang XJ, Vogel H, Roop DR, Bradley A. p63 is a p53 homologue required for limb and epidermal morphogenesis. Nature. 1999;398(6729):708-13.
4. Yang A, Kaghad M, Wang Y, Gillett E, Fleming MD, Dötsch V, et al. p63, a p53 homolog at 3q27-29, encodes multiple products with transactivating, death-inducing, and dominant-negative activities. Mol Cell. 1998;2(3):305-16.
5. Romano RA, Ortt K, Birkaya B, Smalley K, Sinha S. An active role of the DeltaN isoform of p63 in regulating basal keratin genes K5 and K14 and directing epidermal cell fate. PLoS One. 2009;4(5):e5623.
6. Laurikkala J, Mikkola ML, James M, Tummers M, Mills AA, Thesleff I. p63 regulates multiple signalling pathways required for ectodermal organogenesis and differentiation. Development. 2006;133(8):1553-63.
7. Romano RA, Smalley K, Magraw C, Serna VA, Kurita T, Raghavan S, et al. ΔNp63 knockout mice reveal its indispensable role as a master regulator of epithelial development and differentiation. Development. 2012;139(4):772-82.
8. Chakravarti D, Su X, Cho MS, Bui NH, Coarfa C, Venkatanarayan A, et al. Induced multipotency in adult keratinocytes through down-regulation of ΔNp63 or DGCR8. Proc Natl Acad Sci U S A. 2014;111(5):E572-81.
9. Senoo M, Pinto F, Crum CP, McKeon F. p63 Is essential for the proliferative potential of stem cells in stratified epithelia. Cell. 2007;129(3):523-36.
10. Pellegrini G, Dellambra E, Golisano O, Martinelli E, Fantozzi I, Bondanza S, et al. p63 identifies keratinocyte stem cells. Proc Natl Acad Sci U S A. 2001;98(6):3156-61.
11. Koster MI, Kim S, Mills AA, DeMayo FJ, Roop DR. p63 is the molecular switch for initiation of an epithelial stratification program. Genes Dev. 2004;18(2):126-31.
12. Truong AB, Kretz M, Ridky TW, Kimmel R, Khavari PA. p63 regulates proliferation and differentiation of developmentally mature keratinocytes. Genes Dev. 2006;20(22):3185-97.
13. Shalom-Feuerstein R, Lena AM, Zhou H, De La Forest Divonne S, Van Bokhoven H, Candi E, et al. ΔNp63 is an ectodermal gatekeeper of epidermal morphogenesis. Cell Death Differ. 2011;18(5):887-96.
14. Koster MI, Dai D, Marinari B, Sano Y, Costanzo A, Karin M, et al. p63 induces key target genes required for epidermal morphogenesis. Proc Natl Acad Sci U S A. 2007;104(9):3255-60.
15. Parsa R, Yang A, McKeon F, Green H. Association of p63 with proliferative potential in normal and neoplastic human keratinocytes. J Invest Dermatol. 1999;113(6):1099-105.
16. Nylander K, Vojtesek B, Nenutil R, Lindgren B, Roos G, Zhanxiang W, et al. Differential expression of p63 isoforms in normal tissues and neoplastic cells. J Pathol. 2002;198(4):417-27.
17. Keyes WM, Wu Y, Vogel H, Guo X, Lowe SW, Mills AA. p63 deficiency activates a program of cellular senescence and leads to accelerated aging. Genes Dev. 2005;19(17):1986-99.
18. Wolff S, Talos F, Palacios G, Beyer U, Dobbelstein M, Moll UM. The alpha/beta carboxy-terminal domains of p63 are required for skin and limb development. New insights from the Brdm2 mouse which is not a complete p63 knockout but expresses p63 gamma-like proteins. Cell Death Differ. 2009;16(8):1108-17.
19. Soares E, Zhou H. Master regulatory role of p63 in epidermal development and disease. Cell Mol Life Sci. 2018;75(7):1179-90.
20. Rocco JW, Leong CO, Kuperwasser N, DeYoung MP, Ellisen LW. p63 mediates survival in squamous cell carcinoma by suppression of p73-dependent apoptosis. Cancer Cell. 2006;9(1):45-56.
21. Ramsey MR, Wilson C, Ory B, Rothenberg SM, Faquin W, Mills AA, et al. FGFR2 signaling underlies p63 oncogenic function in squamous cell carcinoma. J Clin Invest. 2013;123(8):3525-38.
22. Su X, Napoli M, Abbas HA, Venkatanarayan A, Bui NHB, Coarfa C, et al. TAp63 suppresses mammary tumorigenesis through regulation of the Hippo pathway. Oncogene. 2017;36(17):2377-93.
23. Su X, Paris M, Gi YJ, Tsai KY, Cho MS, Lin YL, et al. TAp63 prevents premature aging by promoting adult stem cell maintenance. Cell Stem Cell. 2009;5(1):64-75.

24. Guo X, Keyes WM, Papazoglu C, Zuber J, Li W, Lowe SW, et al. TAp63 induces senescence and suppresses tumorigenesis in vivo. Nat Cell Biol. 2009;11(12):1451-7.
25. Su X, Chakravarti D, Cho MS, Liu L, Gi YJ, Lin YL, et al. TAp63 suppresses metastasis through coordinate regulation of Dicer and miRNAs. Nature. 2010;467(7318):986-90.
26. Lena AM, Rossi V, Osterburg S, Smirnov A, Osterburg C, Tuppi M, et al. The p63 C-terminus is essential for murine oocyte integrity. Nat Commun. 2021;12(1):383.
27. Fan X, Wang D, Burgmaier JE, Teng Y, Romano RA, Sinha S, et al. Single Cell and Open Chromatin Analysis Reveals Molecular Origin of Epidermal Cells of the Skin. Dev Cell. 2018;47(1):21-37.e5.
28. Napoli M, Wu SJ, Gore BL, Abbas HA, Lee K, Checker R, et al. ΔNp63 regulates a common landscape of enhancer associated genes in non-small cell lung cancer. Nat Commun. 2022;13(1):614.
29. Kouwenhoven EN, van Bokhoven H, Zhou H. Gene regulatory mechanisms orchestrated by p63 in epithelial development and related disorders. Biochim Biophys Acta. 2015;1849(6):590-600.
30. Sethi I, Gluck C, Zhou H, Buck MJ, Sinha S. Evolutionary re-wiring of p63 and the epigenomic regulatory landscape in keratinocytes and its potential implications on species-specific gene expression and phenotypes. Nucleic Acids Res. 2017;45(14):8208-24.
31. Kouwenhoven EN, Oti M, Niehues H, van Heeringen SJ, Schalkwijk J, Stunnenberg HG, et al. Transcription factor p63 bookmarks and regulates dynamic enhancers during epidermal differentiation. EMBO Rep. 2015;16(7):863-78.
32. Venkatanarayan A, Raulji P, Norton W, Chakravarti D, Coarfa C, Su X, et al. IAPP-driven metabolic reprogramming induces regression of p53-deficient tumours in vivo. Nature. 2015;517(7536):626-30.
33. Vasioukhin V, Degenstein L, Wise B, Fuchs E. The magical touch: genome targeting in epidermal stem cells induced by tamoxifen application to mouse skin. Proc Natl Acad Sci U S A. 1999;96(15):8551-6.
34. Dai D, Zhu H, Wlodarczyk B, Zhang L, Li L, Li AG, et al. Fuz controls the morphogenesis and differentiation of hair follicles through the formation of primary cilia. J Invest Dermatol. 2011;131(2):302-10.
35. Rittié L, Tejasvi T, Harms PW, Xing X, Nair RP, Gudjonsson JE, et al. Sebaceous Gland Atrophy in Psoriasis: An Explanation for Psoriatic Alopecia? J Invest Dermatol. 2016;136(9):1792-800.
36. George SM, Taylor MR, Farrant PB. Psoriatic alopecia. Clin Exp Dermatol. 2015;40(7):717-21.
37. Iizuka H, Takahashi H, Honma M, Ishida-Yamamoto A. Unique keratinization process in psoriasis: late differentiation markers are abolished because of the premature cell death. J Dermatol. 2004;31(4):271-6.
38. Buhl AL, Wenzel J. Interleukin-36 in Infectious and Inflammatory Skin Diseases. Front Immunol. 2019;10:1162.
39. Pincelli C. Nerve growth factor and keratinocytes: a role in psoriasis. Eur J Dermatol. 2000;10(2):85-90.
40. Johnston A, Xing X, Wolterink L, Barnes DH, Yin Z, Reingold L, et al. IL-1 and IL-36 are dominant cytokines in generalized pustular psoriasis. J Allergy Clin Immunol. 2017;140(1):109-20.
41. Guttman-Yassky E, Nograles KE, Krueger JG. Contrasting pathogenesis of atopic dermatitis and psoriasis--part I: clinical and pathologic concepts. J Allergy Clin Immunol. 2011;127(5):1110-8.
42. Carroll DK, Carroll JS, Leong CO, Cheng F, Brown M, Mills AA, et al. p63 regulates an adhesion programme and cell survival in epithelial cells. Nat Cell Biol. 2006;8(6):551-61.
43. Ferone G, Mollo MR, Missero C. Epidermal cell junctions and their regulation by p63 in health and disease. Cell Tissue Res. 2015;360(3):513-28.
44. Wang LJ, Li XX, Hou J, Song XH, Xie WH, Shen L. Integrated Analyses of Mouse Stem Cell Transcriptomes Provide Clues for Stem Cell Maintenance and Transdifferentiation. Front Genet. 2020;11:563798.
45. Romano RA, Birkaya B, Sinha S. A functional enhancer of keratin14 is a direct transcriptional target of deltaNp63. J Invest Dermatol. 2007;127(5):1175-86.
46. Clevers H, Loh KM, Nusse R. Stem cell signaling. An integral program for tissue renewal and regeneration: Wnt signaling and stem cell control. Science. 2014;346(6205):1248012.
47. Abe Y, Tanaka N. Roles of the Hedgehog Signaling Pathway in Epidermal and Hair Follicle Development, Homeostasis, and Cancer. J Dev Biol. 2017;5(4).
48. Eckert RL, Adhikary G, Young CA, Jans R, Crish JF, Xu W, et al. AP1 transcription factors in epidermal differentiation and skin cancer. J Skin Cancer. 2013;2013:537028.
49. Nowell C, Radtke F. Cutaneous Notch signaling in health and disease. Cold Spring Harb Perspect Med. 2013;3(12):a017772.

50. Watanabe M, Natsuga K, Nishie W, Kobayashi Y, Donati G, Suzuki S, et al. Type XVII collagen coordinates proliferation in the interfollicular epidermis. Elife. 2017;6.
51. Liu N, Matsumura H, Kato T, Ichinose S, Takada A, Namiki T, et al. Stem cell competition orchestrates skin homeostasis and ageing. Nature. 2019;568(7752):344-50.
52. Matsumura H, Mohri Y, Binh NT, Morinaga H, Fukuda M, Ito M, et al. Hair follicle aging is driven by transepidermal elimination of stem cells via COL17A1 proteolysis. Science. 2016;351(6273):aad4395.
53. Yang R, Liu F, Wang J, Chen X, Xie J, Xiong K. Epidermal stem cells in wound healing and their clinical applications. Stem Cell Res Ther. 2019;10(1):229.
54. Yan S, Ripamonti R, Kawabe H, Ben-Yehuda Greenwald M, Werner S. NEDD4-1 Is a Key Regulator of Epidermal Homeostasis and Wound Repair. J Invest Dermatol. 2021.
55. Zhang X, Yin M, Zhang LJ. Keratin 6, 16 and 17-Critical Barrier Alarmin Molecules in Skin Wounds and Psoriasis. Cells. 2019;8(8).
56. Schonthaler HB, Guinea-Viniegra J, Wculek SK, Ruppen I, Ximénez-Embún P, Guío-Carrión A, et al. S100A8-S100A9 protein complex mediates psoriasis by regulating the expression of complement factor C3. Immunity. 2013;39(6):1171-81.
57. Tian S, Chen S, Feng Y, Li Y. The Interactions of Small Proline-Rich Proteins with Late Cornified Envelope Proteins are Involved in the Pathogenesis of Psoriasis. Clin Cosmet Investig Dermatol. 2021;14:1355-65.
58. Trzeciak M, Sakowicz-Burkiewicz M, Wesserling M, Dobaczewska D, Gleń J, Nowicki R, et al. Expression of Cornified Envelope Proteins in Skin and Its Relationship with Atopic Dermatitis Phenotype. Acta Derm Venereol. 2017;97(1):36-41.
59. Niehues H, Tsoi LC, van der Krieken DA, Jansen PAM, Oortveld MAW, Rodijk-Olthuis D, et al. Psoriasis-Associated Late Cornified Envelope (LCE) Proteins Have Antibacterial Activity. J Invest Dermatol. 2017;137(11):2380-8.
60. Kerkhoff C, Voss A, Scholzen TE, Averill MM, Zänker KS, Bornfeldt KE. Novel insights into the role of S100A8/A9 in skin biology. Exp Dermatol. 2012;21(11):822-6.
61. D'Erme AM, Wilsmann-Theis D, Wagenpfeil J, Hölzel M, Ferring-Schmitt S, Sternberg S, et al. IL-36γ (IL-1F9) is a biomarker for psoriasis skin lesions. J Invest Dermatol. 2015;135(4):1025-32.
62. Albanesi C, Madonna S, Gisondi P, Girolomoni G. The Interplay Between Keratinocytes and Immune Cells in the Pathogenesis of Psoriasis. Front Immunol. 2018;9:1549.
63. Barton CE, Johnson KN, Mays DM, Boehnke K, Shyr Y, Boukamp P, et al. Novel p63 target genes involved in paracrine signaling and keratinocyte differentiation. Cell Death Dis. 2010;1(9):e74.
64. Rasmy H, Mikhael N, Ismail S. Interleukin-18 expression and the response to treatment in patients with psoriasis. Arch Med Sci. 2011;7(4):713-9.
65. Mee JB, Cork MJ, di Giovine FS, Duff GW, Groves RW. Interleukin-1: a key inflammatory mediator in psoriasis? Cytokine. 2006;33(2):72-8.
66. Mitamura Y, Nunomura S, Furue M, Izuhara K. IL-24: A new player in the pathogenesis of pro-inflammatory and allergic skin diseases. Allergol Int. 2020;69(3):405-11.
67. Wang W, Yu X, Wu C, Jin H. IL-36γ inhibits differentiation and induces inflammation of keratinocyte via Wnt signaling pathway in psoriasis. Int J Med Sci. 2017;14(10):1002-7.
68. Gu X, Lundqvist EN, Coates PJ, Thurfjell N, Wettersand E, Nylander K. Dysregulation of TAp63 mRNA and protein levels in psoriasis. J Invest Dermatol. 2006;126(1):137-41.
69. Yin X, Low HQ, Wang L, Li Y, Ellinghaus E, Han J, et al. Genome-wide meta-analysis identifies multiple novel associations and ethnic heterogeneity of psoriasis susceptibility. Nat Commun. 2015;6:6916.
70. Li B, Tsoi LC, Swindell WR, Gudjonsson JE, Tejasvi T, Johnston A, et al. Transcriptome analysis of psoriasis in a large case-control sample: RNA-seq provides insights into disease mechanisms. J Invest Dermatol. 2014;134(7):1828-38.
71. Rizzo JM, Oyelakin A, Min S, Smalley K, Bard J, Luo W, et al. ΔNp63 regulates IL-33 and IL-31 signaling in atopic dermatitis. Cell Death Differ. 2016;23(6):1073-85.
72. Du J, Romano RA, Si H, Mattox A, Bian Y, Yang X, et al. Epidermal overexpression of transgenic ΔNp63 promotes type 2 immune and myeloid inflammatory responses and hyperplasia via NF-κB activation. J Pathol. 2014;232(3):356-68.
73. Jiménez-Andrade Y, Hillette KR, Yoshida T, Kashiwagi M, Choo MK, Liang Y, et al. The Developmental Transcription Factor p63 Is Redeployed to Drive Allergic Skin Inflammation through Phosphorylation by p38α. J Immunol. 2022.

74. Kumar S, Wilkes DW, Samuel N, Blanco MA, Nayak A, Alicea-Torres K, et al. ΔNp63-driven recruitment of myeloid-derived suppressor cells promotes metastasis in triple-negative breast cancer. J Clin Invest. 2018;128(11):5095-109.
75. Ali G, Elsayed AK, Nandakumar M, Bashir M, Younis I, Abu Aqel Y, et al. Keratinocytes Derived from Patient-Specific Induced Pluripotent Stem Cells Recapitulate the Genetic Signature of Psoriasis Disease. Stem Cells Dev. 2020;29(7):383-400.
76. Zhou X, Chen Y, Cui L, Shi Y, Guo C. Advances in the pathogenesis of psoriasis: from keratinocyte perspective. Cell Death Dis. 2022;13(1):81.
77. Jensen KB, Driskell RR, Watt FM. Assaying proliferation and differentiation capacity of stem cells using disaggregated adult mouse epidermis. Nat Protoc. 2010;5(5):898-911.
78. Eyermann CE, Li J, Alexandrova EM. ΔN63 suppresses the ability of pregnancy-identified mammary epithelial cells (PIMECs) to drive HER2-positive breast cancer. Cell Death Dis. 2021;12(6):525.
79. Nemajerova A, Kim SY, Petrenko O, Moll UM. Two-factor reprogramming of somatic cells to pluripotent stem cells reveals partial functional redundancy of Sox2 and Klf4. Cell Death Differ. 2012;19(8):1268-76.

FIGURES AND FIGURE LEGENDS

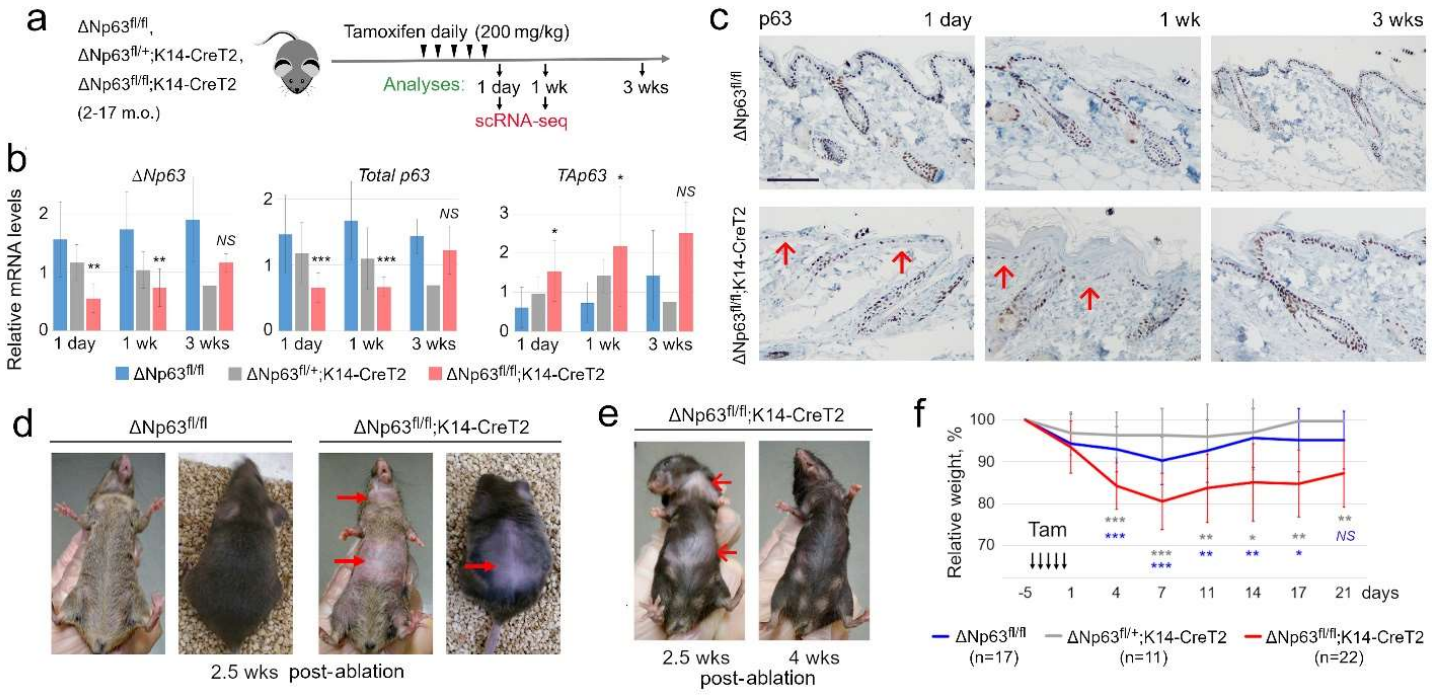

Figure 1. The efficiency and phenotype of ΔNp63 ablation in the adult skin. **a.** Experimental diagram. **b.** qRT-PCR for *ΔNp63*, total *p63* and *TAp63*. **c.** IHC for p63 at the indicated time points, back skin. *Arrows*, interfollicular epidermis with absent p63. Scale bar, 100 μm. **d, e.** Temporary alopecia (*arrows*). **f.** Relative body weight. (**b, f**) Mean ± SD, *p<0.05, **p<0.01, ***p<0.001, *NS*, not significant (**b**, vs. ΔNp63$^{fl/fl}$).

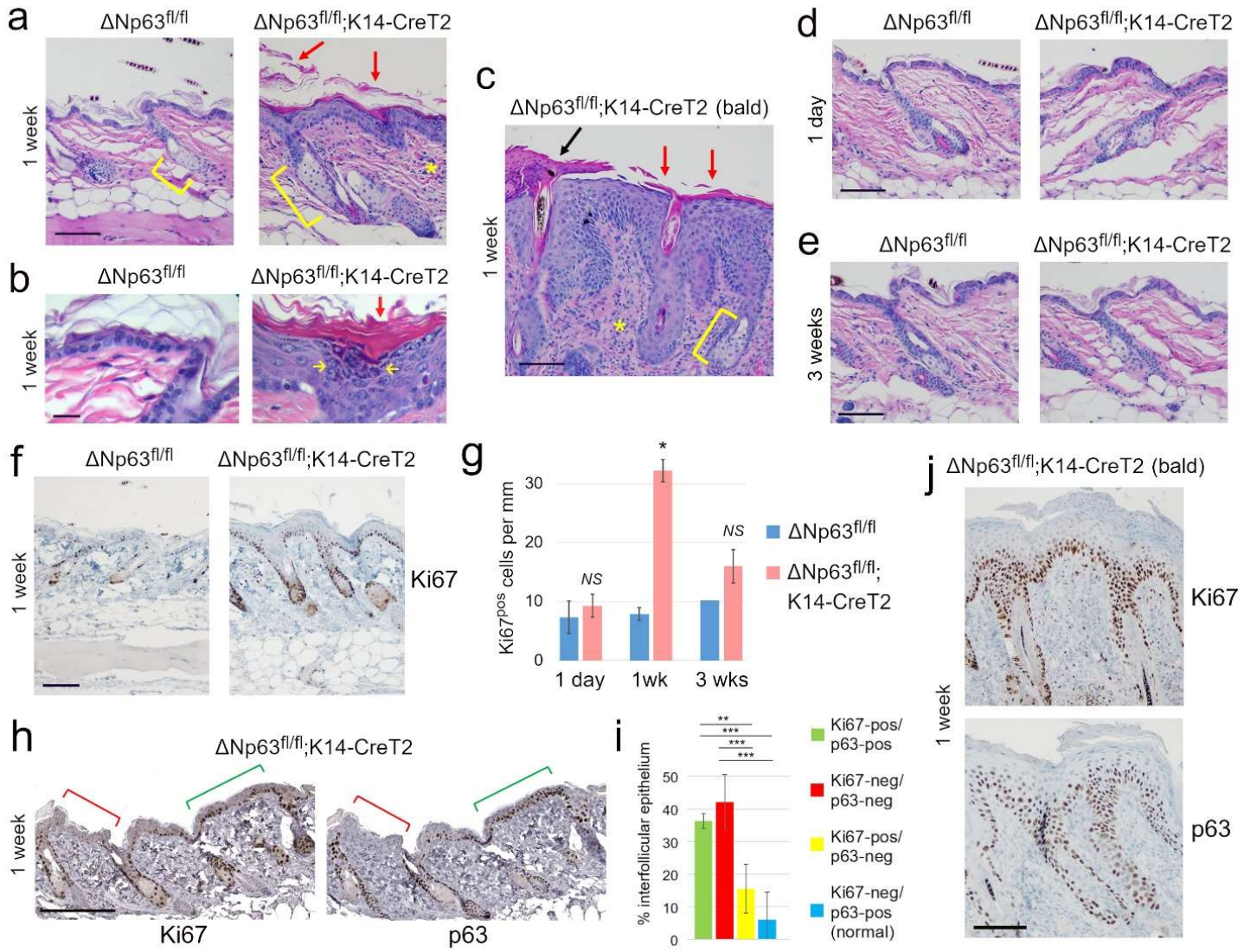

Figure 2. Histopathology and proliferation defects of ΔNp63-ablated skin. **a-e.** H&E at 1 wk post-ablation (**a-c**) showing acanthosis (epidermis thickening), hyperkeratosis (*red arrows*), enlarged keratohyalin granules (*yellow arrows*), parakeratosis (*black arrow*), fibrosis and immune cells infiltration (*asterisks*), and hyperplasia of the sebaceous gland (*brackets*), but no major changes at 1 day (**d**) and 3 wks (**e**) post-ablation. **f, g.** Ki67 IHC (**a**) and quantification (**b**). **h, i.** Ki67 and p63 IHC on serial sections (**h**) and quantification from n=5 mice (**i**). *Red bracket*, $Ki67^{neg}/p63^{neg}$ area; *green bracket*, $Ki67^{pos}/p63^{pos}$ area. **j.** Ki67 and p63 IHC in alopecic skin. "Bald" refers to skin with alopecia. Scale bars, 100 μm (**a, c-e, f, h, j**), 25 μm (**b**). (**g, i**) Mean ± SD, *p<0.05, **p<0.01, ***p<0.001, *NS*, not significant.

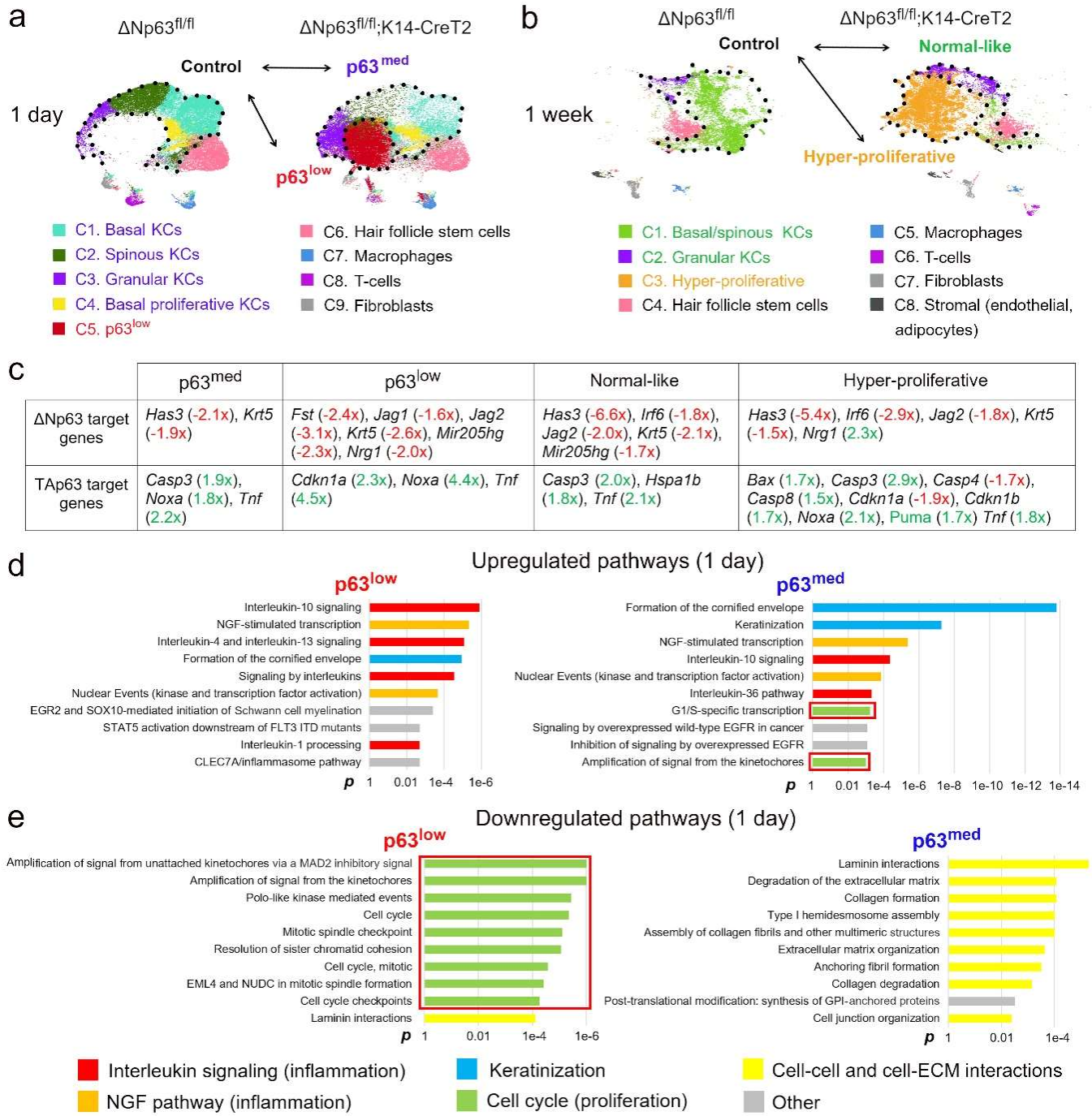

	p63^{med}	p63^{low}	Normal-like	Hyper-proliferative
ΔNp63 target genes	*Has3* (-2.1x), *Krt5* (-1.9x)	*Fst* (-2.4x), *Jag1* (-1.6x), *Jag2* (-3.1x), *Krt5* (-2.6x), *Mir205hg* (-2.3x), *Nrg1* (-2.0x)	*Has3* (-6.6x), *Irf6* (-1.8x), *Jag2* (-2.0x), *Krt5* (-2.1x), *Mir205hg* (-1.7x)	*Has3* (-5.4x), *Irf6* (-2.9x), *Jag2* (-1.8x), *Krt5* (-1.5x), *Nrg1* (2.3x)
TAp63 target genes	*Casp3* (1.9x), *Noxa* (1.8x), *Tnf* (2.2x)	*Cdkn1a* (2.3x), *Noxa* (4.4x), *Tnf* (4.5x)	*Casp3* (2.0x), *Hspa1b* (1.8x), *Tnf* (2.1x)	*Bax* (1.7x), *Casp3* (2.9x), *Casp4* (-1.7x), *Casp8* (1.5x), *Cdkn1a* (-1.9x), *Cdkn1b* (1.7x), *Noxa* (2.1x), Puma (1.7x) *Tnf* (1.8x)

Figure 3. ScRNA-seq of ΔNp63-ablated KCs and the affected molecular pathways. **a.** UMAP plots. At 1 day post-ablation, clusters C1-C4 (collectively, p63^{med}) and C5 (p63^{low}) were separately compared with control clusters C1-C4 to reveal differentially expressed genes and pathways. Similarly, at 1 wk post-ablation, clusters C1-C2 (collectively, "Normal-like") and C3 ("Hyper-proliferative") were separately compared with control clusters C1-C2. **b.** Relative expression levels ΔNp63 and TAp63 target genes in the indicated clusters. **d, e.** The top ten upregulated (**d**) and down-regulated (**e**) pathways at 1 day post-ablation, Reactome.

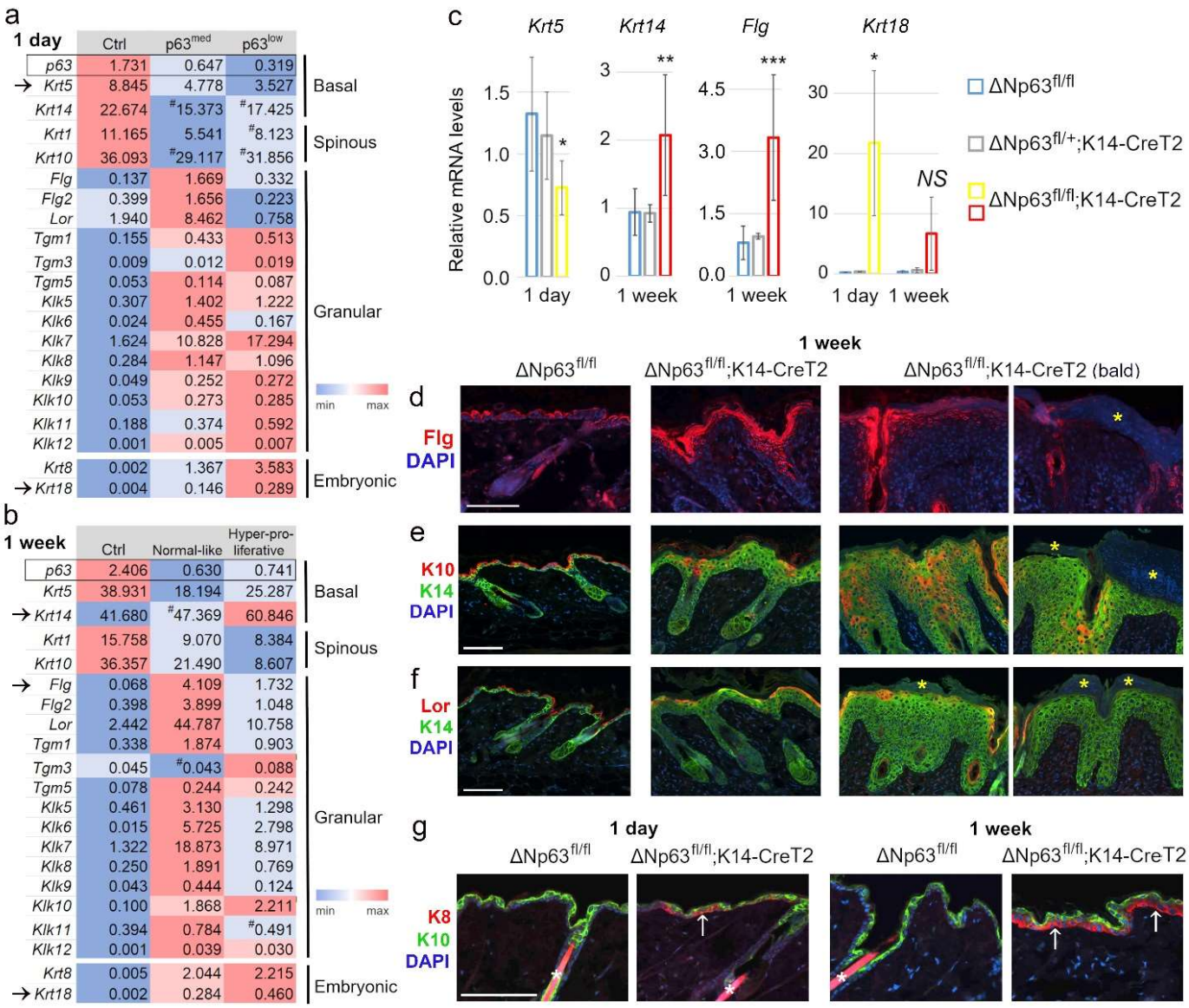

Figure 4. Differentiation defects in ΔNp63-ablated epidermis. **a, b.** Heatmaps of stratification markers at 1 day and 1 wk post-ablation. **c.** Select summary qRT-PCRs of the genes marked with arrows in (**a, b**). Mean ± SD vs. ΔNp63$^{fl/fl}$, *p<0.05, **p<0.01, ***p<0.001, *NS*, not significant. **d-g**. Immunofluorescent staining at 1 wk post-ablation (except **g**). *Asterisks,* parakeratosis corresponding to the areas of lost Flg, K10 and Lor expression. *Arrows*, aberrant Krt8 upregulation; *asterisks*, non-specific hair shaft staining (**g**). Scale bars, 100 μm.

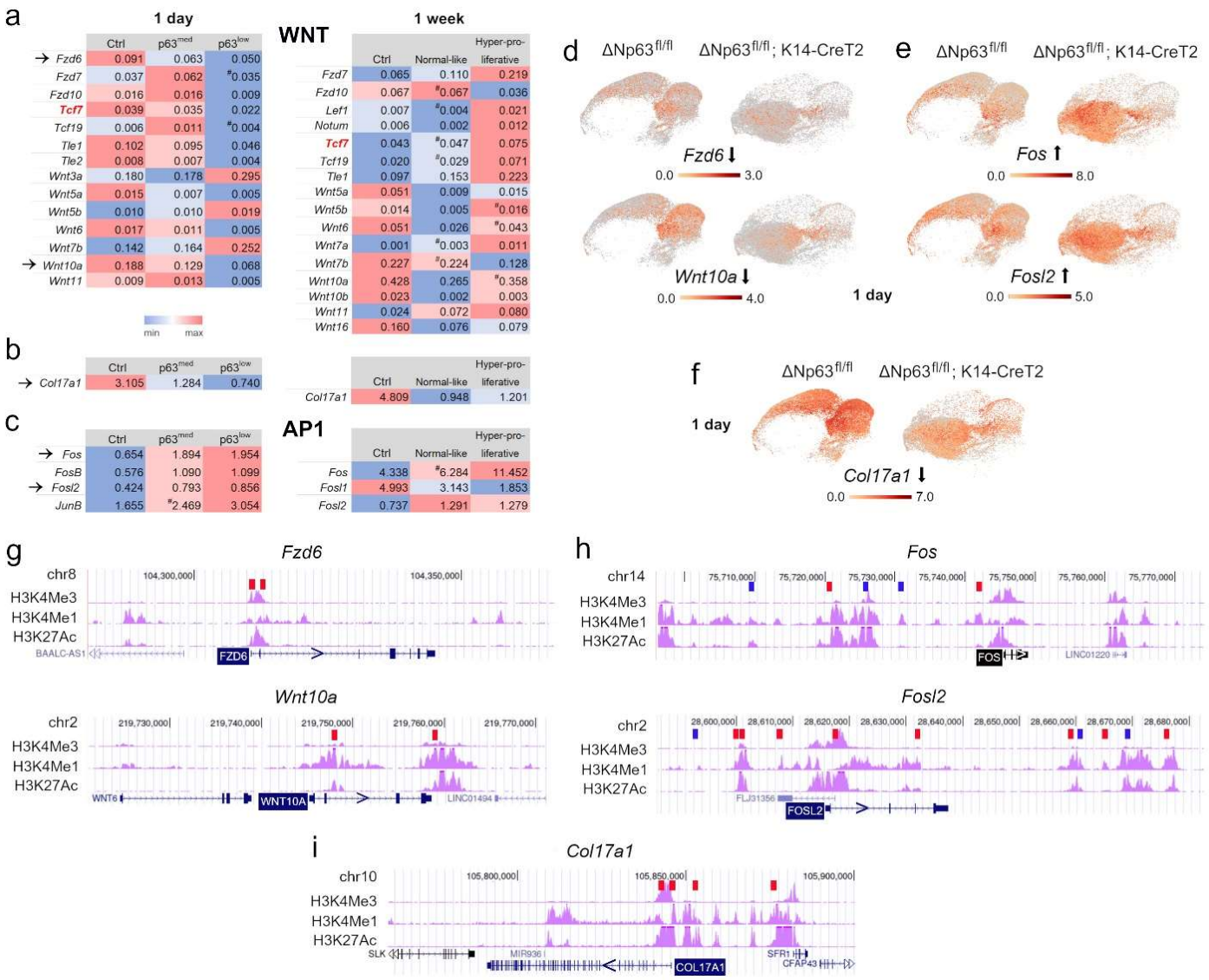

Figure 5. The signaling pathways and genes altered in ΔNp63-ablated KCs. **a-c.** The heatmaps of the differentially expressed genes from the pro-proliferative/pro-stemness Wnt pathway and *Col17a1* (**a, b**) and the pro-differentiation AP1 genes (**c**). *Tcf7* (*red*) is a Wnt target gene and serves as the pathway readout. #, not significant. **d-f.** UMAP plots of the genes marked with arrows in (**a-c**). **g-i.** Potential p63 binding sites in the genes marked with arrows in (**a-c**) inferred from the UCSC genome browser overlayed with chromatin modification tracks (*purple*) and a published p63 CHIP-seq database, both in NHEK cells. *Red*, in all conditions; *blue*, only in proliferative conditions, not to scale.

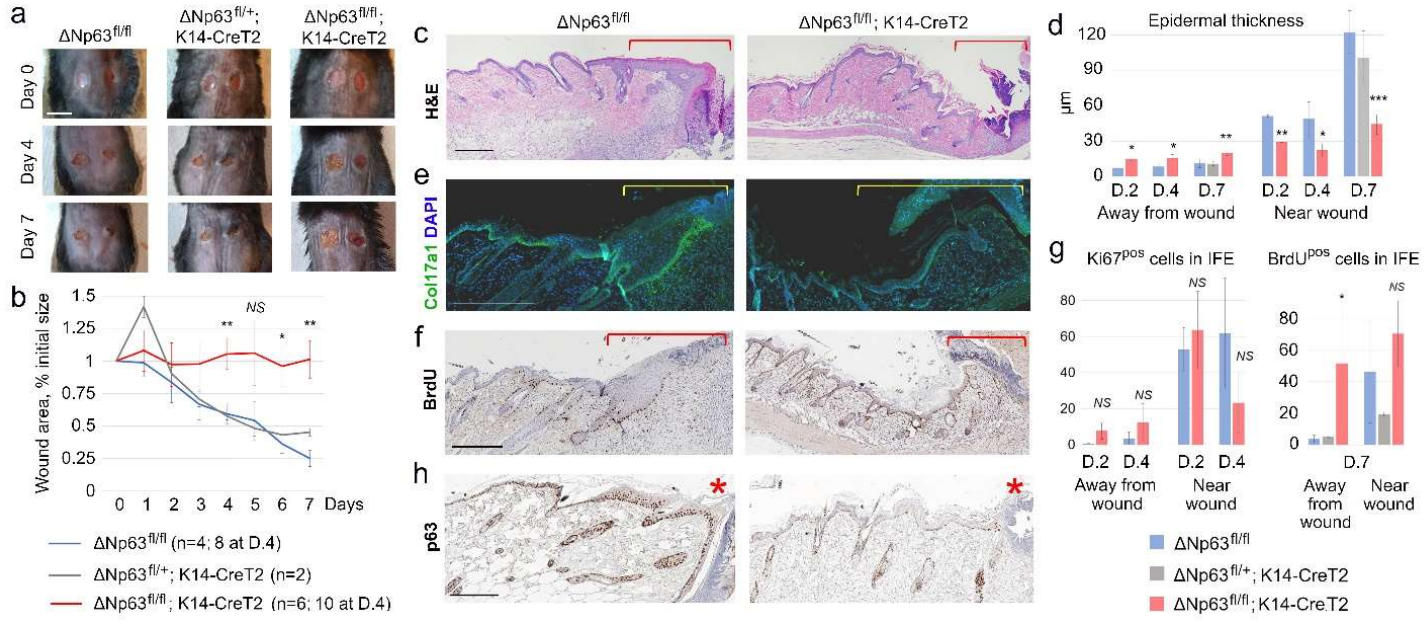

Figure 6. Defective wound healing in ΔNp63-ablated mice. **a, b.** Representative images (**a**) and quantification of the wound area over time (**b**). **c, d**. Impaired formation of the hyper-thickened epidermal ridge, H&E (**c**) and quantification (**d**). **e**. Immunofluorescent staining for Col17a1. **f, g**. IHC for BrdU (**f**) and quantification of Ki67^{pos} (*not shown*) and BrdU^{pos} cells per five interfollicular epidermis (IFE) spaces (**g**). **h**. IHC for p63. All images are at day 7, except **h** (day 4). *Brackets*, *asterisks*, the wound area. (**b, d, g**) Mean ± SD, *p<0.05, **p<0.01, ***p<0.001 with ΔNp63$^{fl/fl}$, *NS*, not significant. Scale bars, 1 cm (**a**), 200 µm (**c, e, f, h**).

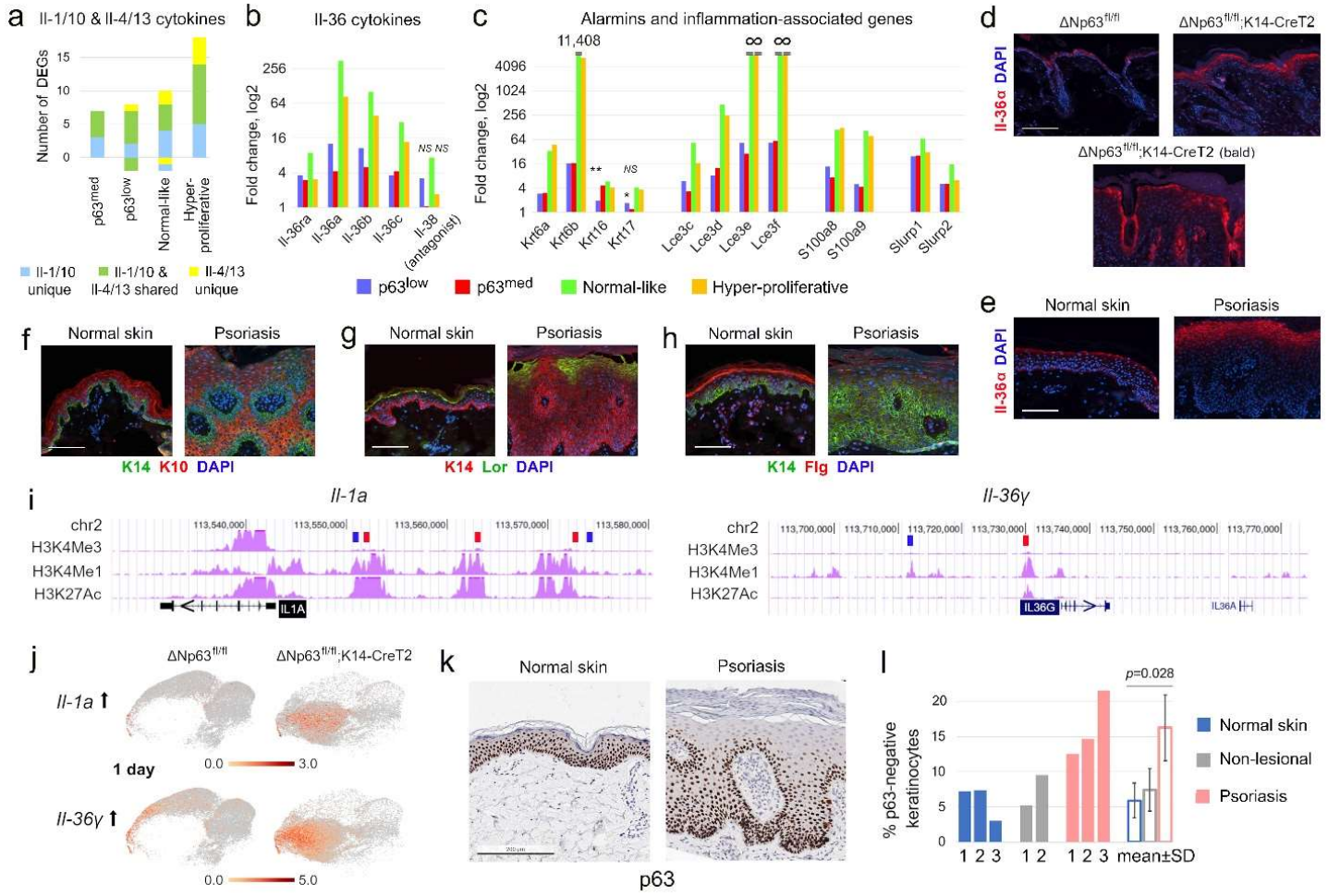

Figure 7. Regulation of inflammation by ΔNp63. **a.** The total number of significantly altered *Il-1/10* and *Il-4/13* genes. **b, c.** Changes in expression levels of *Il-36* genes (**b**) and epidermal alarmins (**c**). **p*<0.05, ***p*<0.01, *NS*, not significant; all others, *p*<0.001. "∞" means the value was divided by zero. **d-h**. Immunofluorescence for the indicated proteins in ΔNp63-ablated mouse skin (**d**) and human biopsies of psoriasis vulgaris (**e-h**). Scale bars, 100 μm. **i, j.** p63 IHC in psoriasis biopsies (**h**) and quantification of $p63^{neg}$ KCs (**i**). Scale bar, 200 μm. **k-n**. UMAP plots (**k, m**) and potential p63 binding sites (**l, n**) in the differentially expressed interleukin genes, inferred from the UCSC genome browser overlayed with chromatin modification tracks (*purple*) and a published p63 CHIP-seq database, both in NHEK cells. *Red*, in all conditions; *blue*, only in proliferative conditions, not to scale.

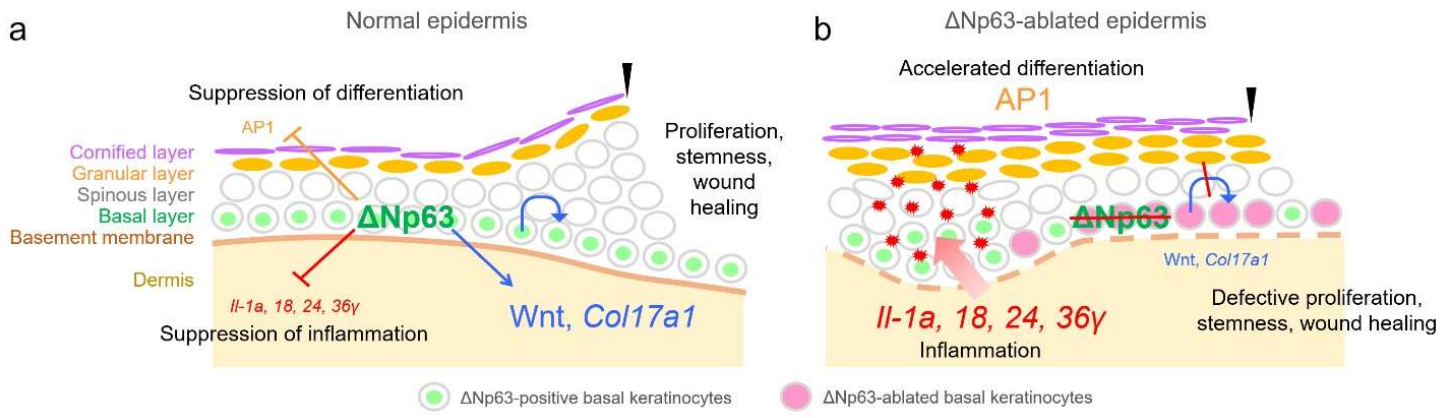

Figure 8. The proposed roles of ΔNp63 in the adult epidermis. **a.** Normal epidermis. **b.** ΔNp63-ablated epidermis. ΔNp63 promotes KC proliferation, stemness and - as a result - wound repair via the Wnt pathway and Col17a1; restricts terminal differentiation via repression of the AP1 factors (collectively, “homeostasis”); represses epidermis-specific inflammatory program by suppressing inflammatory cytokines. The dashed basement membrane designates defective cell-ECM interaction genes, not studied in detail here.

SUPPLEMENTARY MATERIAL

Supplementary Table 1. Frequency of alopecia in ΔNp63-ablated and control adult mice.

	$\Delta Np63^{fl/fl}$	$\Delta Np63^{fl/+}$;K14-CreT2	$\Delta Np63^{fl/fl}$;K14-CreT2
Exp. 1 (4.5 m.o.)	0/8 (0%)	*NA*	5/7 (71%)
Exp. 2 (4.5 m.o.)	0/6 (0%)	*NA*	14/14 (100%)
Exp. 3 (9 m.o.)	0/2 (0%)	*NA*	1/4 (25%)
Exp. 4 (17 m.o.)	0/4 (0%)	*NA*	2/4 (50%)
Exp. 5 (2-5 m.o.)	*NA*	0/1 (0%)	2/3 (67%)
Exp. 6 (8-9 m.o.)	0/4 (0%)	0/4 (0%)	3/3 (100%)
Total	0/24 (0%)	0/5 (0%)	27/35 (77%)

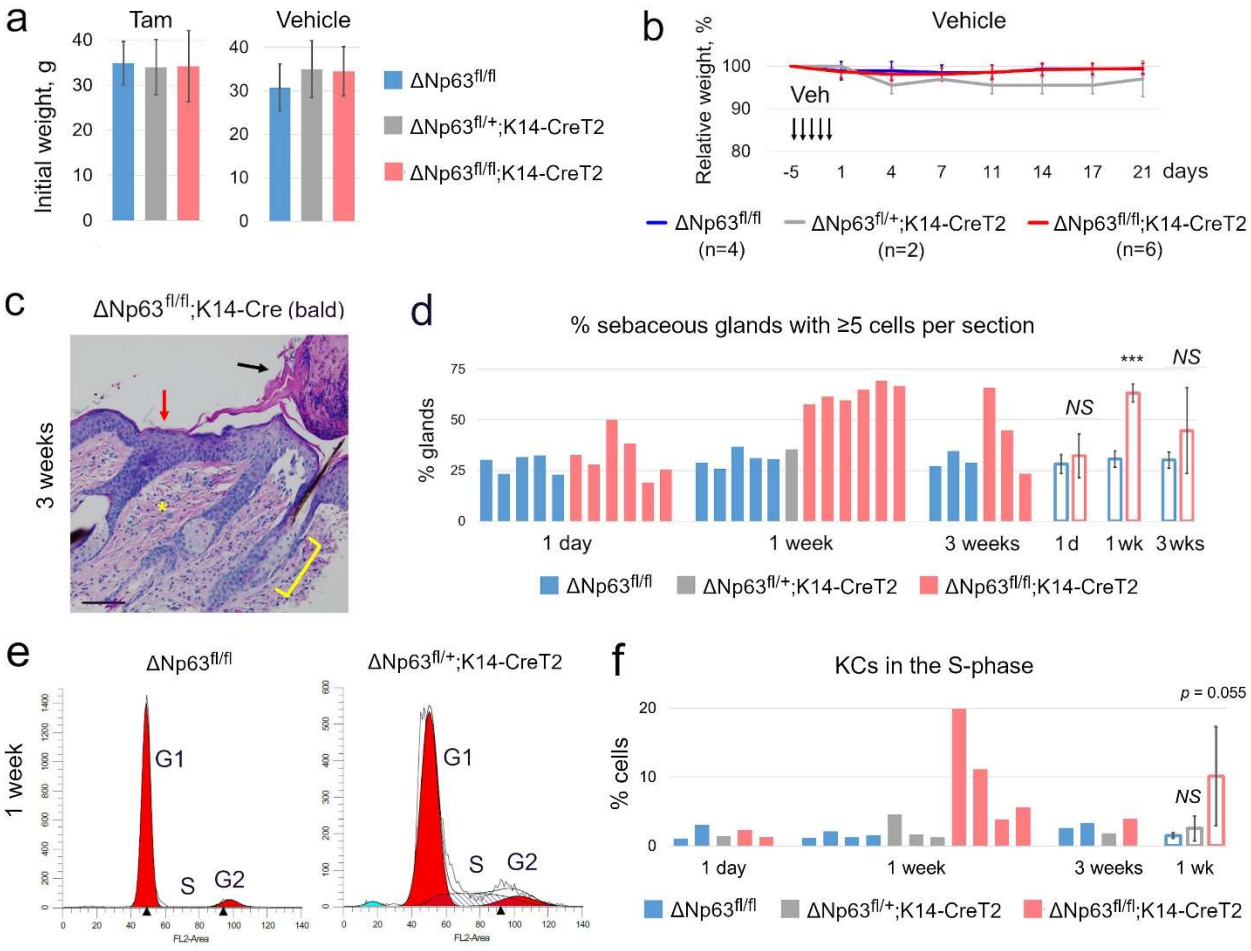

Supplementary Figure 1. Additional phenotypes of ΔNp63-ablated mice. **a, b.** Initial body weight of the indicated genotypes (**a**) and the effect of Vehicle (**b**). **c.** H&E of a rare remaining alopecic ("bald") spot at 3 wks post-ablation showing acanthosis, hyperkeratosis (*red arrow*), parakeratosis (*black arrow*), fibrosis and lymphocytic infiltration (*asterisk*), hyperplasia of the sebaceous gland (*bracket*). Scale bar, 100 μm. **d.** Quantification of the hyperplasia of the sebaceous glands. **e, f.** Cell cycle analysis of isolated back skin keratinocytes, representative histograms (**e**) and quantification (**f**). Open bars are mean ± SD of individual samples at 1 wk post-ablation. ***p<0.001, *NS*, not significant (**d, f**).

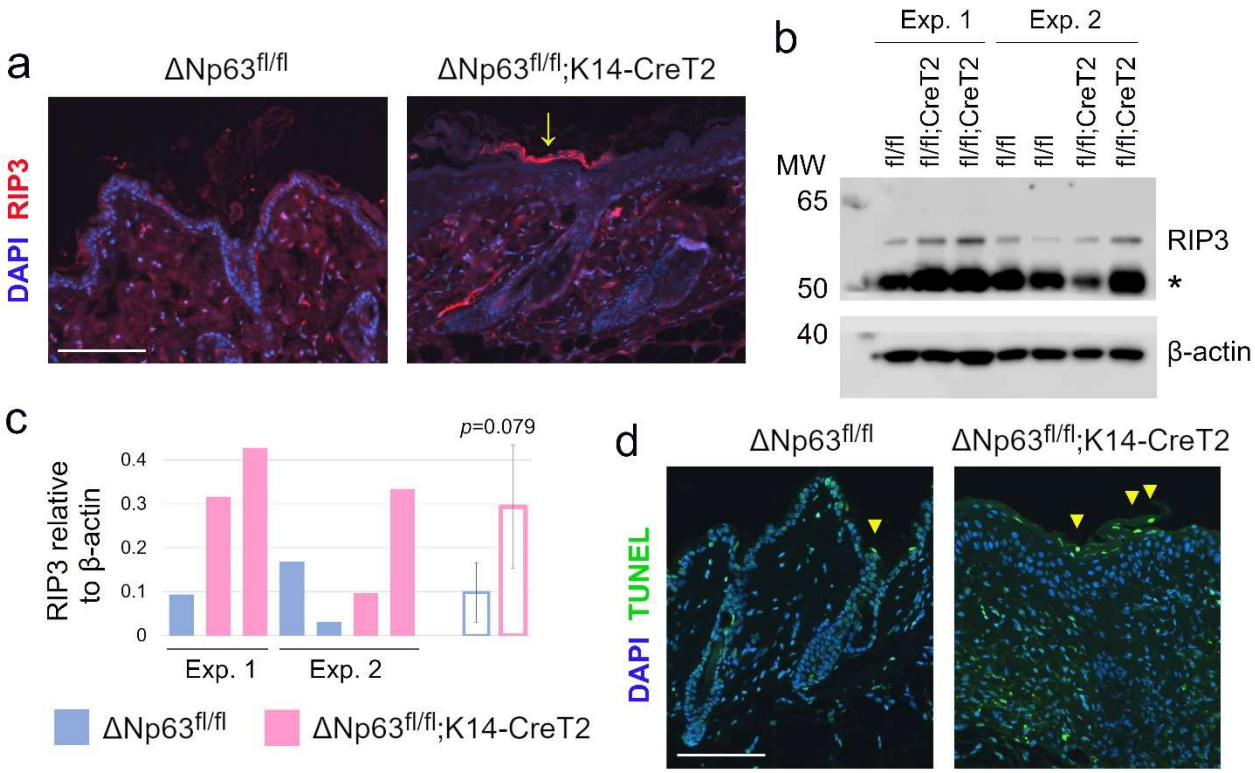

Supplementary Figure 2. Analysis of cell death in ΔNp63-ablated skin. **a-c.** Immunofluorescent staining (**a**), Western blot (**b**) and its quantification (**c**) for a necrosis marker RIP3 at 1 wk post-ablation. *Arrow*, RIP3 upregulation in the outermost epidermal layer (**a**). *, non-specific band (**b**). **d.** The TUNEL assay at 1 wk post-ablation. *Arrowheads*, apoptotic cells in the outermost epidermal layer. Scale bars, 100 μm.

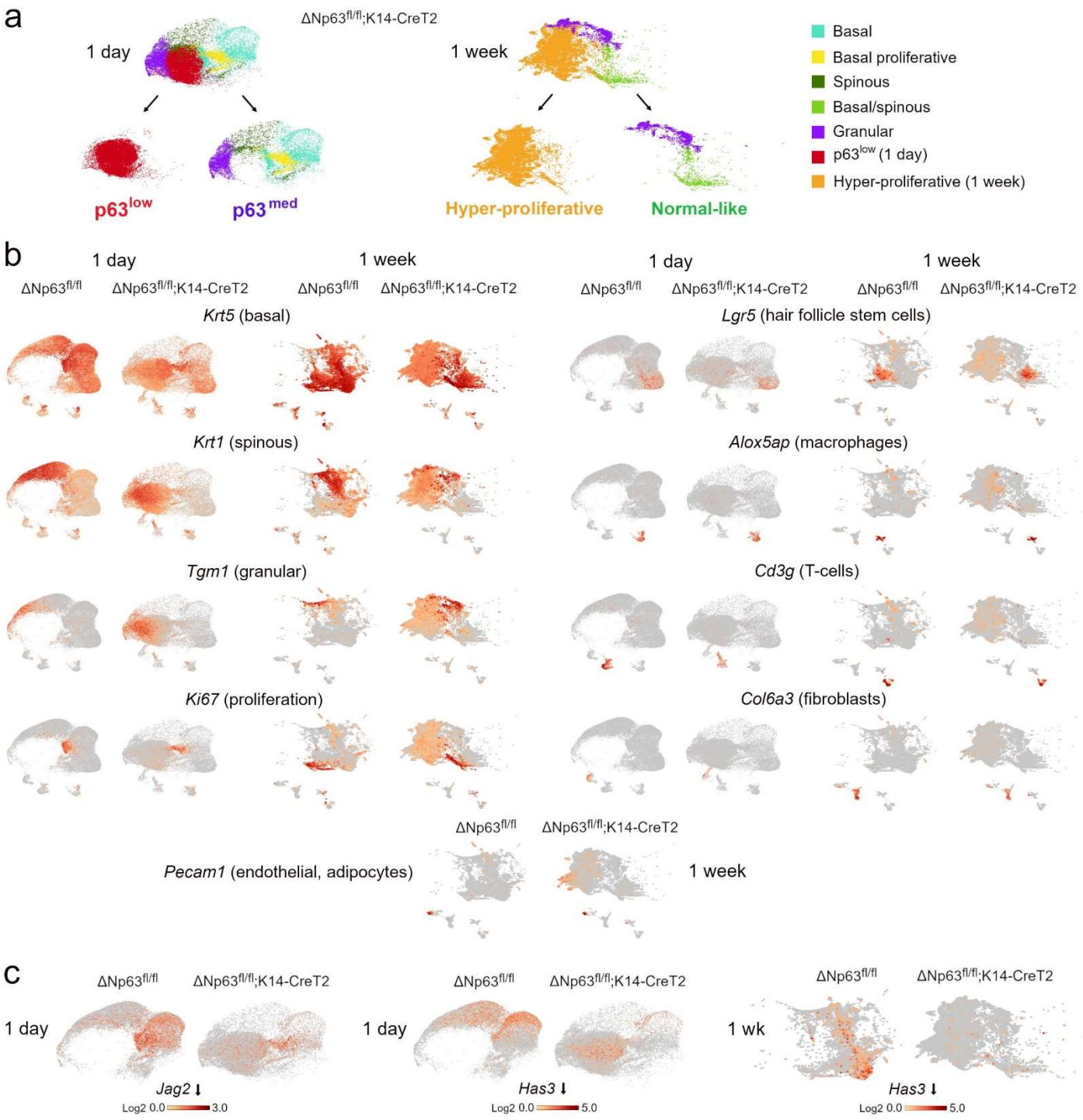

Supplementary Figure 3. Details of scRNA-seq analysis. **a.** Split of the UMAP plots of ΔNp63-ablated KCs at 1 day (*left*) and 1 wk (*right*) post-ablation. **b.** UMAP plots of representative markers used to assign the identity of the clusters. **c.** UMAP plots of select ΔNp63 target genes.

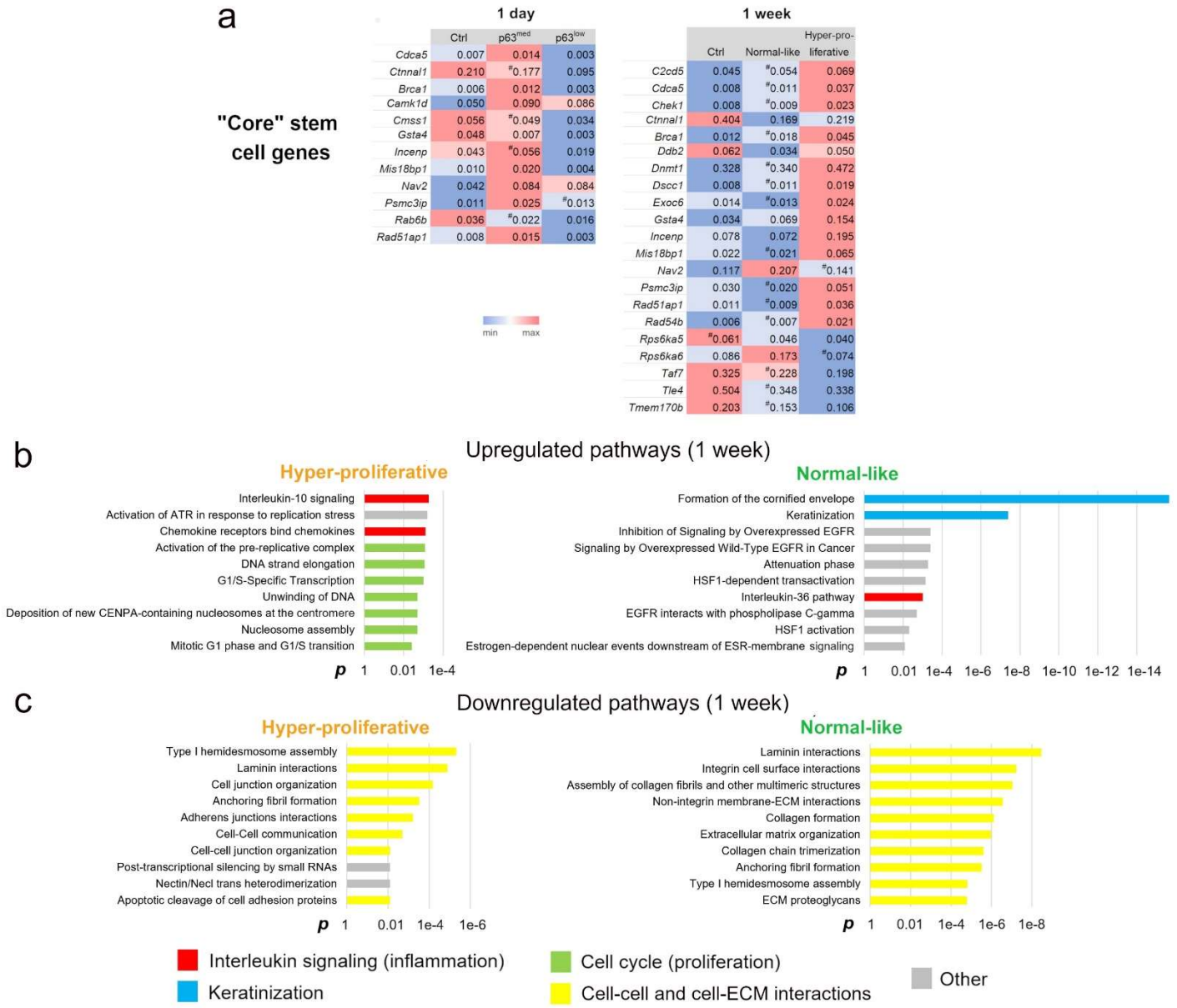

Supplementary Figure 4. Additional differentially regulated genes and pathways. **a.** Heatmaps of previously identified mouse "core" stem cell genes, # not significant. **b, c.** The top ten upregulated (**b**) and down-regulated (**c**) pathways at 1 wk post-ablation, Reactome.

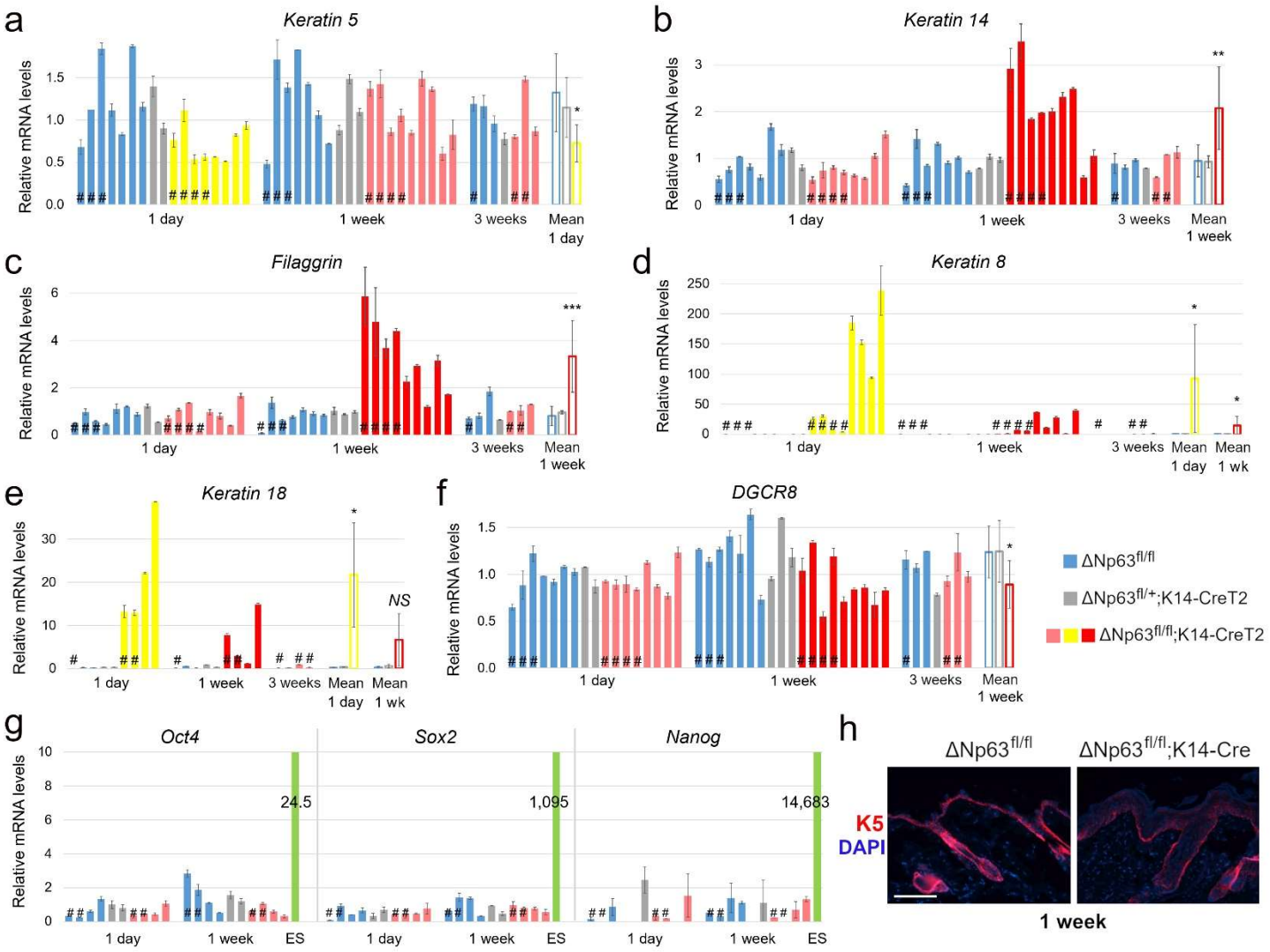

Supplementary Figure 5. Additional gene expression analyses. **a-g.** qRT-PCR of stratification markers (**a-c**), embryonic epidermal genes (**d, e**), *DGCR8* (**f**), and iPSC markers (**g**) on isolated primary KCs, except for # (whole back skin). Mouse ES cells served as a positive control (**g**). Mean ± SD of two technical replicas normalized to *HPRT*. Open bars are mean ± SD of individual samples at the indicated timepoints. *p<0.05, **p<0.01, ***p<0.001, *NS*, not significant. **h.** Immunofluorescent staining of *Krt5*, scale bar, 100 μm.

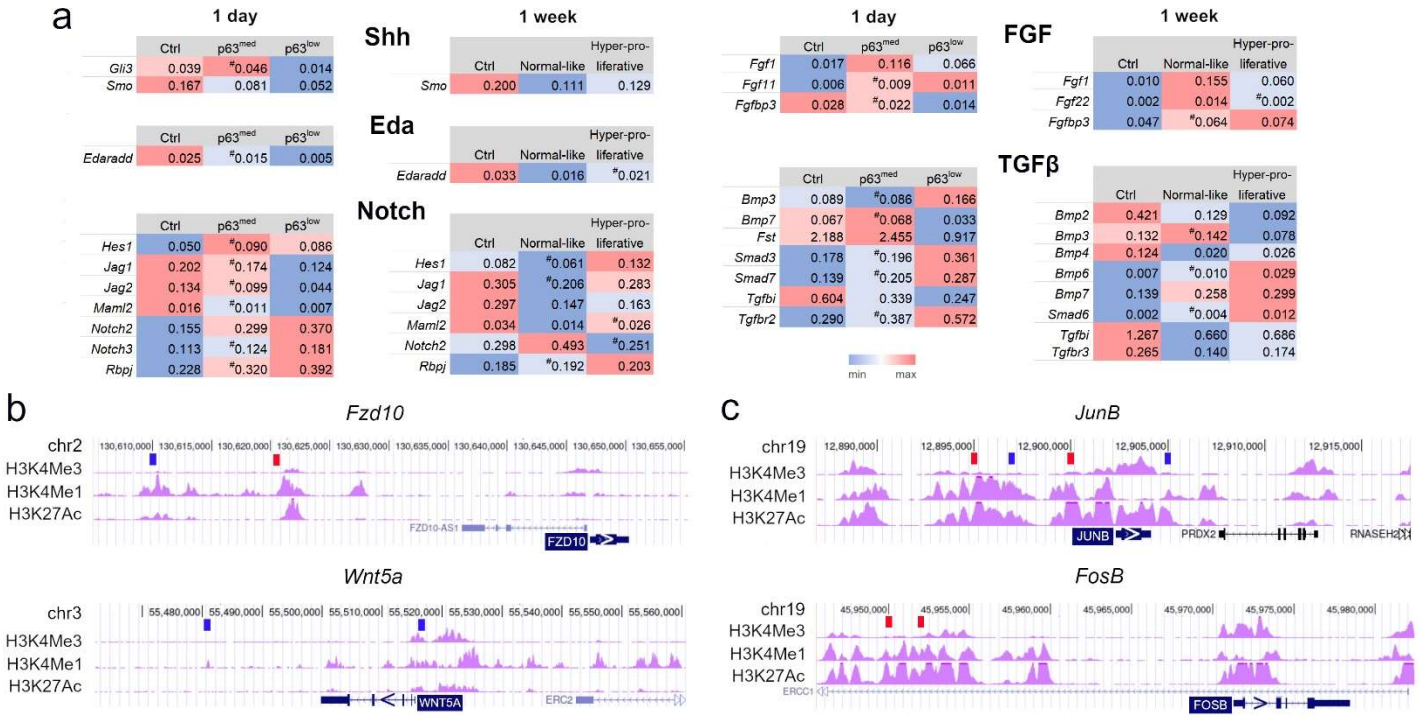

Supplementary Figure 6. Analysis of additional cell signaling pathways and potential ΔNp63-regulated genes. **a.** Heatmaps of the indicated signaling pathways. #, not significant. **b, c.** Potential p63 binding sites in the Wnt pathway genes (**b**) and AP1 factors (**c**); *red*, in all conditions; *blue*, only in proliferative conditions, not to scale.

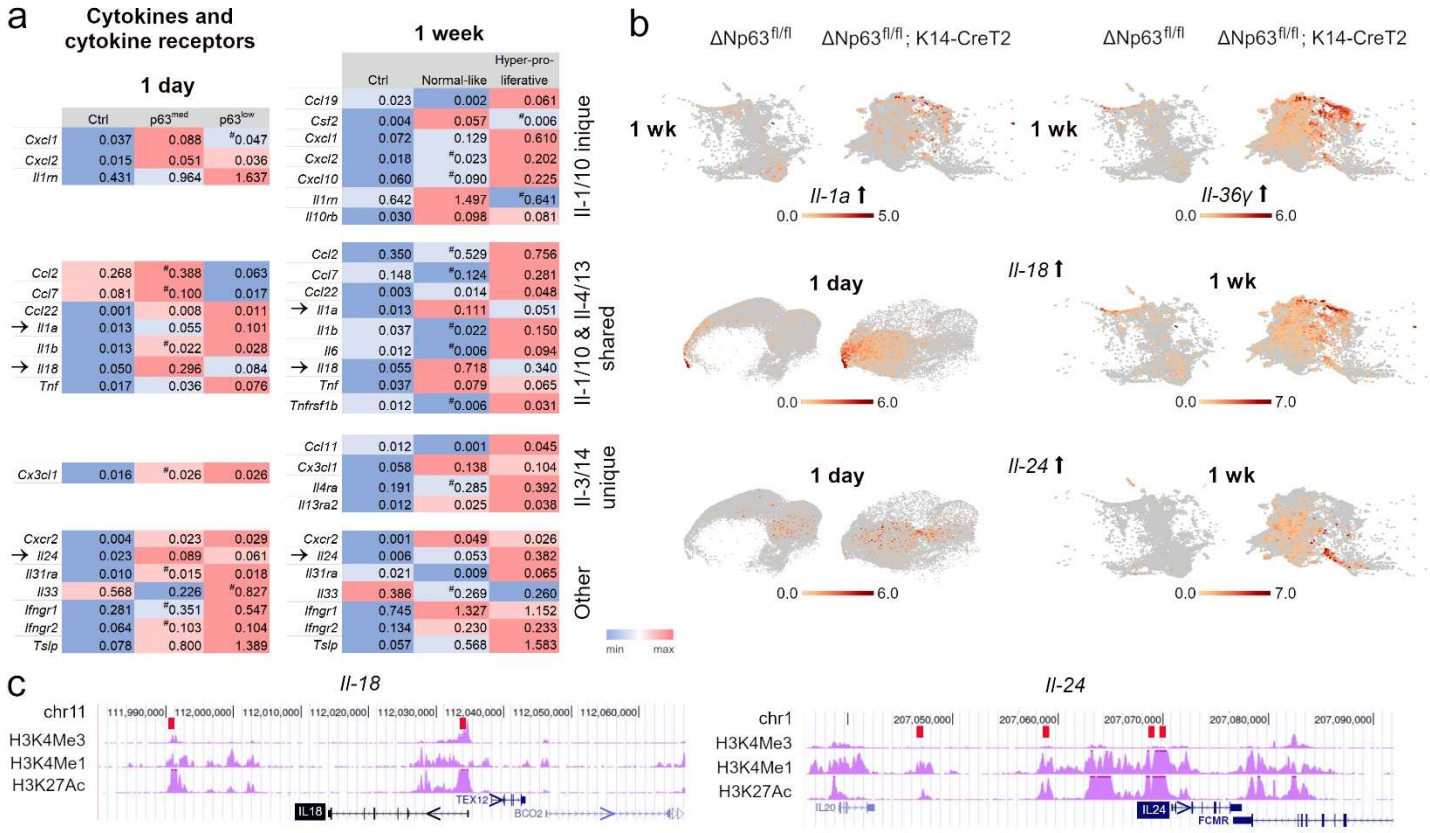

Supplementary Figure 7. Differentially expressed inflammatory cytokines and cytokine receptor genes. **a.** The heatmaps of differentially expressed genes in the indicated pathways. #, not significant. **b.** UMAP plots of the genes marked with arrows in (**a**), see Figure 7j for *Il-1a* and *Il-36γ* at 1 day. **c.** Potential p63 binding sites in *Il-18* and *Il-24* in NHEK cells, not to scale.

SUPPLEMENTARY MATERIALS AND METHODS

Isolation of primary mouse keratinocytes

Primary mouse KCs were isolated as previously described (1) with slight modifications. Mice were euthanized by CO_2 asphyxiation and the back hair removed using hair clippers and Nair hair remover lotion. The skin was washed with 70% ethanol, dissected, and placed the dermal side up on a 10 cm plate on ice, the muscle and adipose tissue was carefully removed with a cell scraper and forceps. The skin was then floated epidermal side up in 10 ml 0.25% trypsin without EDTA (Gibco) either overnight at 4°C or for two hours at 37°C, transferred to a new 10 cm plate, and the epidermal layer was carefully scraped off the dermis using a cell scraper. The epidermis was then minced with a razor blade and clumps were disaggregated by pipetting in trypsin. Ice-cold PBS/10% FBS was added to the cell suspension and passed through a 40 μm mesh. Isolated KCs were gently pelleted and washed twice with ice-cold PBS/10% FBS. Cell number and viability was determined using Trypan blue (Sigma) and the Beckman Coulter Z1 Counter (Beckman Coulter).

Cell cycle analysis

10^6 primary KCs were gently pelleted, washed with ice-cold PBS, fixed in 66% ice-cold ethanol, and stored at 4°C until processing. For analysis, they underwent two rounds of washing and gentle centrifugation, were resuspended in FxCycle PI/RNase Staining Solution (Invitrogen, Waltham, MA) for 15 min. according to the manufacturer's instructions, and were analyzed with a FACSCalibur flow cytometer (BD Biosciences, Franklin Lakes, NJ) and Cyflogic software v1.2.1 (CyFlo Ltd, Turku, Finland).

Additional qRT-PCR primers

DGCR8, Fwd. tacatcgactgtgcacaagg, Rev. gtatgccaagaagaacaggc

Filaggrin, Fwd. ggctccggatactactatg, Rev. gttcgtgctcatgctggtg

Keratin 1, Fwd. ggtctaagttttgggtccg, Rev. aagtctcaggagagagagc

Keratin 5, Fwd. gatccaggttctgctttatg, Rev. accctcaacaacaagtttgc

Keratin 8, Fwd. tgttgtccatgttgctcctc, Rev. tgaacaacaagttcgcctcc

Keratin 10, Fwd. tgtcaatctgcagcagcac, Rev. cgagctggagggtaaaatc

Keratin 14, Fwd. caatctgcatctccaggtc, Rev. ctcctgcagatcgacaatg

Keratin 18, Fwd. agaaatcgaggcactcaagg, Rev. atgatcttgctgaggtcctg

Loricrin, Fwd. cactcatcttccctggtgc, Rev. gagcctcctccagatgagc

Immunohistochemistry, immunofluorescent staining and TUNEL assay

Mice were euthanized and hair was removed using hair clippers and Nair hair remover. Back skin was dissected, fixed in 10% neutral buffered formalin, embedded in paraffin, and sectioned (5 μm). Slides were deparaffinized, rehydrated, and processed for immunohistochemistry (IHC) or immunofluorescent staining. For IHC, slides were boiled in citrate antigen retrieval buffer (Vector Labs, Newark, CA) for 15 min, blocked with 5% NGS (Life Technologies, Carlsbad, CA), and incubated overnight at 4°C with primary antibodies: p63 (1:750, Cell Signaling Technology, Danvers, MA, Cat. #13109), Ki67 (1:400, Cell Signaling Technology, Cat. No. 12202). Slides were washed in PBS and incubated with biotinylated secondary antibody (Invitrogen), followed by Vectastain Elite ABC peroxidase reagent (Vector Labs) and DAB Quanto substrate (Thermo Scientific, Waltham, MA) with hematoxylin counterstain. Additional IHC was done at Histowiz (Brooklyn, NY) with the following antibodies: BrdU (Abcam, Cambridge, UK, Cat. No. ab6326), Ki67 (Abcam, Cat. No. ab15580), p63 (GeneTex, Irvine, CA, Cat. No. GTX102425).

Immunofluorescent staining was performed as previously described (2) with slight modifications. Specifically, antigens were retrieved in sub-boiling buffer (10 mM Tris + 1mM EDTA + 0.05% Tween 20, pH8.0) in a microwave for 20 minutes, then incubated in 5% NGS (Life Technologies) overnight at 4°C with the following primary antibodies: Krt14 (1:800, Biolegend, San Diego, CA), Krt10 (1:200, Biolegend), Lor (1:800, Biolegend), Krt8 (1:300, Millipore, Burlington, MA), Col17a1 (1:250, Abcam, Cat. No. 186415), Il-36α (1:50, Abcam, Cat. No. ab269274), RIP3 (1:100, Santa Cruz Biotechnology, Dallas, TX, Cat. No. sc-374639). After washing in PBS, slides were incubated with fluorescent secondary antibodies. Coverslips were mounted with Prolong Gold with DAPI counterstain (Invitrogen).

The TUNEL assay was done using DeadEnd Fluorometric TUNEL System (Promega, Madison, WI, Cat. No. G3250) according to the manufacturer's instructions. Images were taken with Nikon Eclipse Ti-S microscope (Nikon, Tokyo, Japan) using NIS-Elements AR software (Nikon).

Western blot analysis and quantification

Western blots were performed as previously described (3) using the following primary antibodies: RIP3 (1:500, Santa Cruz Biotechnology, Cat. No. sc-374639), β-actin (1:1000, Santa Cruz Biotechnology, Cat. No. sc-47778). Western blot signals were quantified using the NIH Image software.

SUPPLEMENTARY REFERENCES

1. Jensen KB, Driskell RR, Watt FM. Assaying proliferation and differentiation capacity of stem cells using disaggregated adult mouse epidermis. Nat Protoc. 2010;5(5):898-911.

2. Eyermann CE, Li J, Alexandrova EM. ΔN63 suppresses the ability of pregnancy-identified mammary epithelial cells (PIMECs) to drive HER2-positive breast cancer. Cell Death Dis. 2021;12(6):525.

3. Eyermann CE, Haley JD, Alexandrova EM. The HSP-RTK-Akt axis mediates acquired resistance to Ganetespib in HER2-positive breast cancer. Cell Death Dis. 2021;12(1):126.